Mechanisms Underlying the Synchronizing Action of Corticothalamic Feedback Through Inhibition of Thalamic Relay Cells

ALAIN DESTEXHE, DIEGO CONTRERAS, AND MIRCEA STERIADE
Laboratoire de Neurophysiologie, Faculté de Médecine, Université Laval, Québec G1K 7P4, Canada

Destexhe, Alain, Diego Contreras, and Mircea Steriade. Mechanisms underlying the synchronizing action of corticothalamic feedback through inhibition of thalamic relay cells. *J. Neurophysiol.* 79: 999–1016, 1998. Early studies have shown that spindle oscillations are generated in the thalamus and are synchronized over wide cortical territories. More recent experiments have shown that this large-scale synchrony depends on the integrity of corticothalamic feedback. Previously proposed mechanisms emphasized exclusively intrathalamic mechanisms to generate the synchrony of these oscillations. In the present paper, we propose a cellular mechanism in which the synchrony is dependent of a mutual interaction between cortex and thalamus. This cellular mechanism is tested by computational models consisting of pyramidal cells, interneurons, thalamic reticular (RE) and thalamocortical (TC) relay cells, on the basis of voltage-clamp data on intrinsic currents and synaptic receptors present in the circuitry. The model suggests that corticothalamic feedback must operate on the thalamus mainly through excitation of GABAergic RE neurons, therefore recruiting relay cells essentially through inhibition and rebound. We provide experimental evidence for such dominant inhibition in the lateral posterior nucleus. In these conditions, the model shows that cortical discharges optimally evoked thalamic oscillations. This feature is essential to the present cellular mechanism and is also consistently observed experimentally. The model further shows that, with this type of corticothalamic feedback, cortical discharges recruited large areas of the thalamus because of the divergent cortex-to-RE and RE-to-TC axonal projections. Consequently, the thalamocortical network generated patterns of oscillations and synchrony similar to in vivo recordings. The model also emphasizes the important role of the modulation of the I_h current by calcium in TC cells. This property conferred a relative refractoriness to the entire network, a feature also observed experimentally, as we show here. Further, the same property accounted for various spatiotemporal features of oscillations, such as systematic propagation after low-intensity cortical stimulation, local oscillations, and more generally, a high variability in the patterns of spontaneous oscillations, similar to in vivo recordings. We propose that the large-scale synchrony of spindle oscillations in vivo is the result of thalamocortical interactions in which the corticothalamic feedback acts predominantly through the RE nucleus. Several predictions are suggested to test the validity of this model.

INTRODUCTION

Since early studies (Morison and Bassett 1945), it is known that sleep spindle oscillations survive decortication and are generated within the thalamic circuitry. In a detailed experimental and theoretical analysis of these oscillations, Andersen and colleagues proposed a cellular mechanism that consisted in a mutual recruitment of thalamocortical (TC) relay cells and thalamic local-circuit inhibitory interneurons on the basis of the rebound property of TC cells (Andersen and Andersson 1968; Andersen and Sears 1964). Later, in

vivo experiments demonstrated the critical involvement of the GABAergic neurons from the reticular (RE) nucleus of the thalamus rather than local-circuit interneurons (Steriade et al. 1985). The deafferented rostral pole of the RE nucleus was even shown to generate spindle rhythmicity by itself in vivo (Steriade et al. 1987).

The investigation of spindle oscillations in ferret lateral geniculate slices (Bal et al. 1995a,b; von Krosigk et al. 1993) demonstrated a mechanism similar to that proposed initially by Andersen and colleagues, with a critical role for the rebound burst and a mutual recruitment of TC and RE cells. The latter played the same role as the local-circuit interneurons in Andersen's model, although the properties and connectivity of these two types of inhibitory cells are different. Moreover, these in vitro spindle waves were shown to behave as traveling waves (Kim et al. 1995) after a mechanism of progressive recruitment resulting from intrathalamic axonal projections, a mechanism also proposed earlier by Andersen et al. (Andersen and Andersson 1968; Andersen et al. 1967).

After the characterization of the ionic currents underlying the rebound burst in thalamic cells (Huguenard and Prince 1992; Jahnsen and Llinás 1984) and the synaptic receptors present in thalamic circuits (von Krosigk et al. 1993), detailed biophysical models of interacting thalamic neurons have been designed. These models proposed an explanation for the observation of rhythmicity in the deafferented RE nucleus in vivo (Destexhe et al. 1994a; Golomb et al. 1994). An explanation for the absence of oscillations in the isolated RE nucleus in vitro (von Krosigk et al. 1993) was proposed on the basis of the depolarizing effect of noradrenaline and serotonin that may be necessary to maintain oscillations (Destexhe et al. 1994b).

Although these hypothetical mechanisms proposed a plausible explanation for the above data, there are still a number of experimental observations left unexplored. First, spindles recorded in the cortex in vivo showed that oscillations appeared ''nearly simultaneously'' in different cortical sites (Contreras et al. 1997a; near-simultaneity is defined here by the temporal overlap of oscillations in different leads during most of the spindle sequence), a feature also typical of human sleep spindles (Bremer 1958; Contreras et al. 1997a). Second, spindle waves recorded in thalamic slices, show a ''systematic propagation'' from one side to the other of the slice (Kim et al. 1995; systematic propagation is defined here as a systematic pattern of initiation between two different sites, such that the initiation delay is progressively larger for sites of increasing distances). In this case, distant sites rarely oscillated in unison (see Figs. 1–2 in Kim et al. 1995), which is clearly different from in vivo recordings in

which the entire recorded area oscillated in unison during most of the spindle sequence (see Figs. 1–2 in Contreras et al. 1997a). Third, near-simultaneous spindle waves were also evidenced by multielectrode thalamic recordings of anesthetized cats in vivo (Contreras et al. 1997a). In this case, the large-scale synchrony was disrupted by removal of the cerebral cortex (Contreras et al., 1996a). Clearly, intrathalamic synchronizing mechanisms seems insufficient to account for the large-scale synchrony of oscillations in vivo.

Yielding further insight into this question requires to take into account the influence of the cortex. As already proposed by Morison and Dempsey (1943), the neocortex was shown to powerfully trigger spindle oscillations (Contreras and Steriade 1996; Roy et al. 1984; Steriade et al. 1972). Deep cortical incisions had no measurable effect on the synchrony of oscillations, suggesting a limited role of intracortical connections, and further emphasizing the role of corticothalamic feedback in large-scale synchrony (Contreras et al. 1996a). It must be noted, however, that the synchrony between hemispheres is reduced in cats after section of the corpus callosum (see Andersen and Andersson 1968), suggesting that at least some intracortical connections are important.

In the present paper, we propose and analyze a mechanism in which all the above in vivo and in vitro observations find a plausible explanation. By contrast to previously proposed mechanisms for spindle oscillations, which always involved exclusively intrathalamic synchronizing mechanisms, we propose here a cellular mechanism for large-scale synchrony that consists in a mutual recruitment of the thalamus and cortex. We show that this mechanism holds only if corticothalamic feedback acts predominantly on exciting RE cells, therefore recruiting TC cells via dominant inhibition.

METHODS

Computational models of intrinsic currents

Single compartment models were constructed for cortical pyramidal cells (PY), cortical interneurons (IN), and thalamic TC and RE cells. Models were modified versions from previous models (Destexhe et al. 1996b; McCormick et al. 1993). The minimal set of currents needed to reproduce spindle oscillations and their properties were integrated in the models.

Every cell was described by the membrane equation

$$C_m \dot{V}_i = - g_L (V_i - E_L) - \sum_j I_{ji}^{int} - \sum_k I_{ki}^{syn} \qquad (1)$$

where V_i is the membrane potential, $C_m = 1 \ \mu F/cm^2$ is the specific capacity of the membrane, g_L is the leakage conductance and E_L is the leakage reversal potential. Intrinsic and synaptic currents are respectively represented by I_{ji}^{int} and I_{ki}^{syn}.

Intrinsic currents were described by the generic form

$$I_{ji}^{int} = \bar{g}_j m_j^M h_j^N (V_i - E_j) \qquad (2)$$

where the current is expressed as the product of respectively the maximal conductance, $\bar{g}_j$, activation (m_j) and inactivation variables (h_j), and the difference between the membrane potential V_i, and the reversal potential E_j. Activation and inactivation gates follow the simple two-state kinetic scheme introduced by Hodgkin and Huxley (1952)

$$(closed) \ \underset{\beta(V)}{\overset{\alpha(V)}{\rightleftarrows}} \ (open) \qquad (3)$$
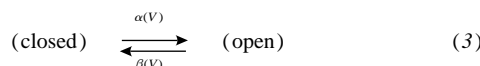
where α and β are voltage-dependent rate constants.

The set of intrinsic currents was different for each cell type and

TABLE 1. *Parameters intrinsic to each cell type in the model*

Parameter (Membrane Area)	Value
Cortical pyramidal cells (PY)	
	29,000 μm^2
$\bar{g}_L$	0.1 mS/cm^2
E_L	−70 mV
$\bar{g}_{Na}$	50 mS/cm^2
$\bar{g}_K$	5 mS/cm^2
$\bar{g}_M$	0.07 mS/cm^2
Cortical interneurons (IN)	
	14,000 μm^2
g_L	0.15 mS/cm^2
E_L	−70 mV
$\bar{g}_{Na}$	50 mS/cm^2
$\bar{g}_K$	10 mS/cm^2
Thalamic reticular cells (RE)	
	14,000 μm^2
$\bar{g}_L$	0.05 mS/cm^2
E_L	−90 mV
$\bar{g}_{Na}$	200 mS/cm^2
$\bar{g}_K$	20 mS/cm^2
$\bar{g}_{Ts}$	3 mS/cm^2
Thalamocortical cells (TC)	
	29,000 μm^2
$\bar{g}_L$	0.01 mS/cm^2
E_L	−70 mV
$\bar{g}_{KL}$	3–5* nS
$\bar{g}_{Na}$	90 mS/cm^2
$\bar{g}_K$	10 mS/cm^2
$\bar{g}_T$	2 mS/cm^2
$\bar{g}_h$	0.015–0.02* mS/cm^2

* Extreme values used to randomize the properties of TC cells.

for each current, parameter values were obtained from matching the kinetic model to voltage-clamp data. The intrinsic currents used here and references for more details were: I_T and I_h in TC cells (Destexhe et al. 1996a; Huguenard and McCormick 1992; McCormick and Huguenard 1992), I_T in RE cells (Destexhe et al. 1996b), I_M in PY cells (McCormick et al. 1993) and, for all cells, I_{Na}-I_K currents responsible for action potentials (Traub and Miles, 1991). In TC and RE cells, Ca^{2+} dynamics and all other parameters were identical to a previous model (Destexhe et al. 1996a). Parameters for intrinsic currents and passive properties are summarized in Table 1.

The intrinsic properties of thalamic and cortical cells in the model are summarized in Fig. 1 (Intrinsic). Because of the presence of I_T current, both types of thalamic cell could produce bursts of action potentials. In TC cells, in addition to I_T, the presence of I_h conferred oscillatory properties and the upregulation of I_h by intracellular Ca^{2+} led to waxing-and-waning properties of these oscillations, as detailed in previous models (Destexhe et al. 1993a,b and 1996a). Models for cortical excitatory (PY) and inhibitory (IN) cells were kept as simple as possible and were derived from previous models (McCormick et al. 1993). Because of the presence of I_M, excitatory neurons generated adapting trains of action potentials, similar to "regular spiking" pyramidal cells (Connors and Gutnick 1990), and inhibitory interneurons had no other current than those necessary to generate action potentials ("fast spiking" cells).

All cells of the same type had homogeneous conductance parameters in the network, except for TC cells. Our hypothesis is that

several initiation sites for oscillations occur in the thalamus because of the heterogeneity of TC cells (see text). Many TC cells are spontaneous oscillators, as observed in thalamic slices (Leresche et al. 1991; McCormick and Pape 1990) and in vivo (Curró Dossi et al. 1992). If TC cells are modeled with different values of I_h conductance, a few of these cells will be intrinsic oscillators. In models, this minority of TC cells play the role of ''initiator'' for spindle oscillations (see Destexhe et al. 1996a). In the present network, several initiator TC cells were present because of randomization of I_h and leak potassium (I_{KL}) conductances (see Table 1).

Thalamic refractoriness (Kim et al. 1995) is a reduced tendency of TC cells to display rebound bursts, because of an activity-dependent enhancement of the I_h current (Bal and McCormick 1996). Intracellular Ca^{2+} was proposed as a likely candidate for this modulatory role of I_h in thalamic neurons (Destexhe et al. 1993a; McCormick 1992; Toth and Crunelli 1992), similarly to sinoatrial node cells (Hagiwara and Irisawa 1989). This modulation of I_h was evidenced recently in thalamic neurons from caged Ca^{2+} experiments (Luthi and McCormick, 1997; but see Budde et al., 1997). A Ca^{2+}-dependent modulation of I_h was explored in modeling studies of spindle oscillations in thalamic circuits (Destexhe et al. 1993b, 1996a). In the present model, I_h was regulated by intracellular Ca^{2+} using a kinetic model involving Ca^{2+}-binding proteins, identical to a previous study (Destexhe et al. 1996a). The action of Ca^{2+} was to lock the I_h channels in the open state, resulting in a shift of the activation curve to more depolarized values, as observed experimentally (Hagiwara and Irisawa 1989). The kinetics of this modulation was adjusted to reproduce the slow ADP in TC cells (Destexhe et al. 1996a); the rates for unbinding of Ca^{2+} were comparable with the rates observed in other systems (Legendre et al. 1993).

Models of synaptic currents and receptors

Synaptic currents were described by

$$I_{ki}^{syn} = \bar{g}_{ki} m_{ki} (V_i - E_{ki}) \qquad (4)$$

where ki indicates the synaptic contact from neuron k to neuron i, $\bar{g}_{ki}$ is the maximal conductance of postsynaptic receptors and E_{ki} is the reversal potential. m_{ki} is the fraction of open receptors according to the simple two-state kinetic scheme (Destexhe et al. 1994b)

$$(closed) + T(V_k) \underset{\beta}{\overset{\alpha}{\rightleftarrows}} (open)$$
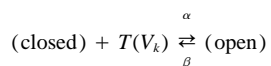
where $T(V_k)$ is the concentration of transmitter in the cleft. When a spike occurred in cell k, $T(V_k)$ was set to 0.5 mM during 0.3 ms, leading to the transient activation of the current. Receptor types such as α-amino-3-hydroxy-5-methyl-4-isoxazolepropionic acid (AMPA) and γ-aminobutyric acid-A ($GABA_A$) were described by two-state kinetic models for the activation variable m, whereas $GABA_B$ receptors had a more complex activation scheme based on the kinetics of G proteins (see details in Destexhe and Sejnowski 1995; Destexhe et al. 1996a).

AMPA receptors were mediating all excitatory connections in this model. Simulations with N-methyl-D-aspartate (NMDA) currents did not show any appreciable difference. A mixture of $GABA_A$ and $GABA_B$ receptors mediated all inhibitory synaptic interaction, except within the RE nucleus, where $GABA_A$ receptors mediate the majority of synaptic interactions between RE cells (Bal et al. 1995b; Ulrich and Huguenard 1996). In the model, removing $GABA_B$ receptors had no effect on synchrony and phase relations between cells, but changed the precise time of onset of the spindle. They were therefore kept in this study.

On the basis of whole cell recordings of hippocampal pyramidal cells for $GABA_A$ (Otis and Mody 1992), $GABA_B$ (Otis et al. 1993), and AMPA (Xiang et al., 1992) responses, we designed simple kinetic models to represent the typical time course of these

currents (Destexhe et al. 1994b, 1998). As the present modeling study is based on experimental data obtained mostly in barbiturate-anesthetized animals (pentobarbital) and that barbiturates prolong the decay time course of $GABA_A$ currents (Thompson 1994), we have used a different decay time constant for $GABA_A$. Application of pentobarbital in hippocampal slices slows down the normal rate of decay, about 5 ms, to about 7–25 ms, but the amplitude of the current remains unaffected (reviewed in Thompson 1994). We used here a rate of decay of 12.5 ms, which lies in the middle of that range. This slower $GABA_A$ current also provided inhibitory postsynaptic potentials (IPSPs) with a time course close to that seen in intracellular recordings in animals anesthetized with pentobarbital (e.g., Contreras and Steriade 1996; Steriade and Deschênes 1984). The time course of postsynaptic potentials are summarized in Fig. 1 (Synaptic).

Facilitation or depression of EPSPs and IPSPs do exist in thalamus (Deschênes and Hu 1990; Steriade and Deschênes 1984; Thompson and West 1991) but were not incorporated in this model.

Network structure and synaptic connections

Morphological studies have shown that ascending thalamocortical fibers give most of their synaptic contacts in layers I, IV, and VI of the cerebral cortex (White 1986). Given that layer VI pyramidal neurons constitute the major source of corticothalamic fibers, these cells therefore mediate a monosynaptic excitatory feedback loop (thalamus-cortex-thalamus) (Hersch and White 1981; White and Hersch 1982). This is also demonstrated by thalamically evoked antidromic and monosynaptic responses in the same, deeply lying cortical cell (see Fig. 5 in Steriade et al. 1993b). Although all thalamic projecting layer VI pyramidal cells leave axon collaterals in the RE nucleus, some lower layer V pyramids also project to thalamic nuclei, but do not leave collaterals in the RE nucleus (Bourassa and Deschênes 1995). The latter were not modeled. We did not include either the influence of some thalamic intralaminar nuclei that project diffusely to the cerebral cortex as well as receive projections from it (Jones 1985). We have considered here a simple one-dimensional network of excitatory and inhibitory cortical cells to model this layer VI network. This one-dimensional network model with two cell types is a greatly simplified representation of the multilayered structure of the cortex but no additional complexity was needed for the purpose of the present work.

In area 5 of cat cerebral cortex, axon collaterals from pyramidal cells are profuse and dense but remain localized within a few hundreds of microns (Avendaño et al. 1988). The connections of cells in the two layers of the cortical network were organized such that each PY or IN cell projected densely to a localized area of about 10% of the size of the network (11 cells; Fig. 4, *scheme*), centered on each presynaptic cell. The same size of projection was also assumed for intrathalamic connections (see below).

The structure of the thalamus was approximated by a two layer one-dimensional network, including one layer of TC cells and one layer of RE cells. As there is evidence that thalamic interneurons do not play a role in generation of spindle oscillations (Steriade et al. 1985; von Krosigk et al. 1993), they were not incorporated. On the basis of anatomic data showing that axonal projections in the thalamic circuitry are local and topographic (FitzGibbon et al. 1995; Jones 1985; Minderhoud 1971), each thalamic cell type made topographic axonal connections with other cell types, with a projection size of about 10% of the size of the network (11 cells; see Fig. 4, *scheme*). These thalamic connection patterns were identical to a previous model (Destexhe et al. 1996a).

Projections between thalamus and cortex are also topographic (Avendaño et al. 1985; Jones 1985; Robertson and Cunningham 1981; Updyke 1981) but have more divergence than intrathalamic or intracortical connections (Bourassa and Deschênes 1995; Freund et al. 1989; Landry and Deschênes 1981; Rausell and Jones 1995).

As schematized in Fig. 4, each PY cell projected to 21 RE and 21 TC cells, twice the extent of intrathalamic and intracortical projections. Similarly, each TC cell projected topographically to 21 PY and 21 IN cells with uniform synaptic weights.

All axonal projections of a given type were identical in extent from cell to cell and all synaptic conductances were equal. The total synaptic conductance on each neuron was the same for cells of the same type, independently of the size of the network. Reflexive boundary conditions were used to minimize boundary effects (see Destexhe et al. 1994a, 1996a). Conductance values are given in Table 2.

Synaptic bombardment

In some simulations (Fig. 9), cortical pyramidal cells were subject to random synaptic bombardment to mimic properties of the network in vivo. In this case, every PY cell had 40 extra synapses (20 AMPA and 20 GABA$_A$) with conductance values of 0.01 μS and 0.0025 μS for each AMPA and GABA$_A$ synapse, respectively. These extra synapses received random presynaptic action potentials computed with a Poisson generator of spikes (Press et al. 1986), with an average frequency of 15 Hz. This random synaptic bombardment of excitatory postsynaptic potentials (EPSPs) and IPSPs produced a fluctuating voltage trace in PY cells with occasional spontaneous firing. These features were similar to our in vivo intracellular recordings during light barbiturate anesthesia.

Variability with parameters

A possible difficulty of network simulations is the variability with parameters. Parameters were estimated as follows. Intrinsic current kinetics were estimated from voltage-clamp data in thalamic and cortical cells; in some cases, the relative conductance of each current could also be estimated from the literature. The kinetics of synaptic currents are also known from whole cell recordings in thalamic, hippocampal, and cortical cells and were integrated in the models; the synaptic currents in the present model were directly fit to experimental recordings. The current-clamp behavior of single cells was compared to experimental data, which is an important check for the validity of the parameter values used. Finally, the synaptic weights are the most difficult parameter to estimate because models are usually of a much smaller scale than the actual thalamocortical networks.

Various experimental data are available for a rough estimation of these parameters, such as the EPSP/IPSP size in various cells after extracellular stimulation. For example, compared to cortical stimulation, thalamic stimulation evokes very powerful EPSPs in intracellularly recorded PY cells in vivo (D. Contreras and M. Steriade, unpublished observations). In intracellularly recorded TC cells in vivo, cortical stimulation results in a small amplitude EPSP followed by a large IPSP (Fig. 2A).

Network simulations can be sensitive to synaptic conductance parameters. It is therefore important to vary these parameters to test their effect at the network level. The variability of parameters intrinsic to the thalamic circuitry was checked in a previous paper (Destexhe et al. 1996a) and was not repeated here. The same parameters were used with the important exception that TC cell properties were randomly distributed to allow several initiation sites in the network.

With conductance parameters defined appropriately, the behavior of a small thalamocortical circuit (such as in Fig. 3) can be compared to that of larger networks (as in Fig. 4). The parameter definition was the total synaptic conductance per cell (the sum over all individual synaptic conductances of the same connection type). An extensive search of the synaptic conductance parameter space was done by using the small thalamocortical circuit. The values obtained for the domain corresponding to spindle oscillations are given in the last column of Table II. A large number of

TABLE 2. *Total synaptic conductances used for each type of connection*

Type of Receptor	Location	Optimal Conductance Value	Range Tested
AMPA	PY → PY	0.6 μS	0–0.9 μS
AMPA	PY → IN	0.2 μS	0.1–0.4 μS
GABA$_A$	IN → PY	0.15 μS	0.09–0.2 μS
GABA$_B$	IN → PY	0.03 μS	0–0.2 μS
AMPA	TC → RE	0.2 μS	0.1–1 μS*
GABA$_A$	RE → RE	0.2 μS	0.05–0.4 μS*
GABA$_A$	RE → TC	0.02 μS	0.01–0.04 μS*
GABA$_B$	RE → TC	0.04 μS	0–0.15 μS*
AMPA	TC → PY	1.2 μS	0.4–2.5 μS
AMPA	TC → IN	0.4 μS	0.1–0.6 μS
AMPA	PY → RE	1.2 μS	0.4–2 μS
AMPA	PY → TC	0.01 μS	0–0.07μS

Each value represents sum of all individual synaptic conductances of the same type converging to a given cell. Range of conductance values indicated gives rise to similar oscillations as the optimal value. * Range tested in Destexhe et al. 1996a. AMPA, amino-3-hydroxy-5-methyl-4-isoxazolepropionic acid; GABA, γ-aminobutyric acid; PY, cortical pyramidal cells; IN, cortical interneurons; RE, thalamic reticular cells; TC, thalamocortical cells.

simulations ($n = 125$) were run for equivalent parameter values in the large network to check for robustness. Surprisingly, few differences were seen between the circuit and large network's behavior. The differences were presumably the result of the randomization of I_h conductance in TC cells. The range indicated in Table II is therefore also valid for the network model, although differences may be seen close to the extreme values given in the table.

Besides the fact that each conductance parameter needed to be within some range of values to sustain spindling behavior, some parameters were found to be critical. One example is the intracortical GABA$_A$-mediated inhibition that need to be above some level to prevent avalanches of discharges in the system and epileptic-like behavior. Another critical parameter was the conductance of AMPA-mediated cortical feedback in TC and RE cells. This parameter is at the center of focus of the present study and is discussed in detail in the RESULTS section.

All simulations were done with the use of NEURON (Hines and Carnevale 1997) on a Sparc 20 workstation (Sun Microsystems, Mountain View, CA).

Intracellular and field potential recordings

In vivo recordings were obtained from adult cats anesthetized with pentobarbital (35 mg/kg). Intracellular recordings were obtained in TC cells from the lateral posterior nucleus. Methods for intracellular recordings were described in detail in Contreras and Steriade 1995, 1996. Glass micropipettes were filled with 3M potassium acetate and had final DC resistances of 30–40 MΩ. Stimulation were done using bipolar electrodes inserted in the depth of the suprasylvian cortex.

Multisite local field potentials (LFPs) were recorded from the suprasylvian gyrus. The procedures for multisite LFPs were described in detail in Contreras et al. (1997a). The spatial coherence was evaluated by computing the spatial correlation in the thalamus similarly to Methods described in Contreras et al. (1996a).

RESULTS

We start by describing the model and its main mechanism, namely that corticothalamic feedback operates essentially by feedforward inhibition on TC cells. We provide experimental

evidence for this mechanism and show with the model how it can account for the spatial and temporal properties of spindle oscillations.

The building blocks of the thalamocortical network are single compartment models of interconnected thalamic and cortical cells described by the same models as in Destexhe et al. (1996a) for thalamic cells and simplified models of cortical cells. Cortical pyramidal (PY) cells were of the ''regular-spiking'' type with voltage-dependent currents I_M, I_{Na} and I_K (McCormick et al. 1993; see METHODS). Cortical inhibitory (IN) interneurons were of the fast-spiking type (Connors and Gutnick 1990) with only I_{Na} and I_K as voltage-dependent currents. All currents were described by Hodgkin-Huxley type of kinetics and synaptic currents were described by kinetic models (Destexhe et al. 1998) for AMPA, GABA$_A$, and GABA$_B$ receptors; NMDA receptors were not included. Intrinsic properties, synaptic potentials and schemes of connectivity are summarized in Fig. 1.

IPSP dominance in thalamocortical cells

We first illustrate experimental evidence supporting one of the key properties explored in this study, namely that corticothalamic feedback operates on the thalamus mainly by exciting RE cells, therefore recruiting TC cells through IPSPs that dominate over direct cortical EPSPs. There are no quantitative data for the strength of cortical EPSPs on TC and RE cells. However, intracellular recordings of RE cells consistently show a high sensitivity to EPSPs of cortical origin and produce bursts of action potentials in response to electrical stimulation of the anatomically related cortical area, even with low stimulus intensities (Contreras et al. 1993; Mulle et al. 1986). The same feature was observed from internal capsule stimulation in thalamic slices (Thomson and West 1991). On the other hand, intracellular recordings of TC cells, while stimulating the anatomically related cortical area, show an EPSP-IPSP sequence clearly dominated by the IPSP component (Fig. 2A). This case represented the vast majority of recorded TC cells in the lateral posterior nucleus (24 of 26) with measured IPSP amplitudes of 11.1 ± 1.2 mV (mean ± SE) at −60 mV ($n = 26$). In some cases ($n = 5$), no trace of EPSP could be observed while IPSPs were always present. That cortical stimulation was able to fire the TC cell through EPSPs was only occasionally observed ($n = 2$) at the resting membrane potential (−62.3 ± 1.5 mV).

Possible mechanisms for such IPSP dominance in TC cells were investigated from simulation of thalamic networks. In a small circuit of 2 TC interconnected with 2 RE cells (see scheme in Fig. 2B), simulated EPSPs on RE and TC cells could reproduce the EPSP/IPSP sequence seen experimentally provided cortical EPSPs on RE cells were considerably more effective than EPSPs on TC cells. In Fig. 2B, the conductance of AMPA-mediated cortical drive on TC and RE cells, as well as the GABA$_A$-mediated IPSP from RE cells were of the same order of magnitude. In this case, cortical EPSPs were shunt by reticular IPSPs and cortical stimulation did not evoke oscillations in the thalamic circuit. On the other hand, when EPSPs on TC cells had smaller conductance (5 nS compared with 100 nS), the EPSP-IPSP sequence was similar to intracellular recordings and cortical stimulation was very effective to evoke oscillations (Fig. 2C).
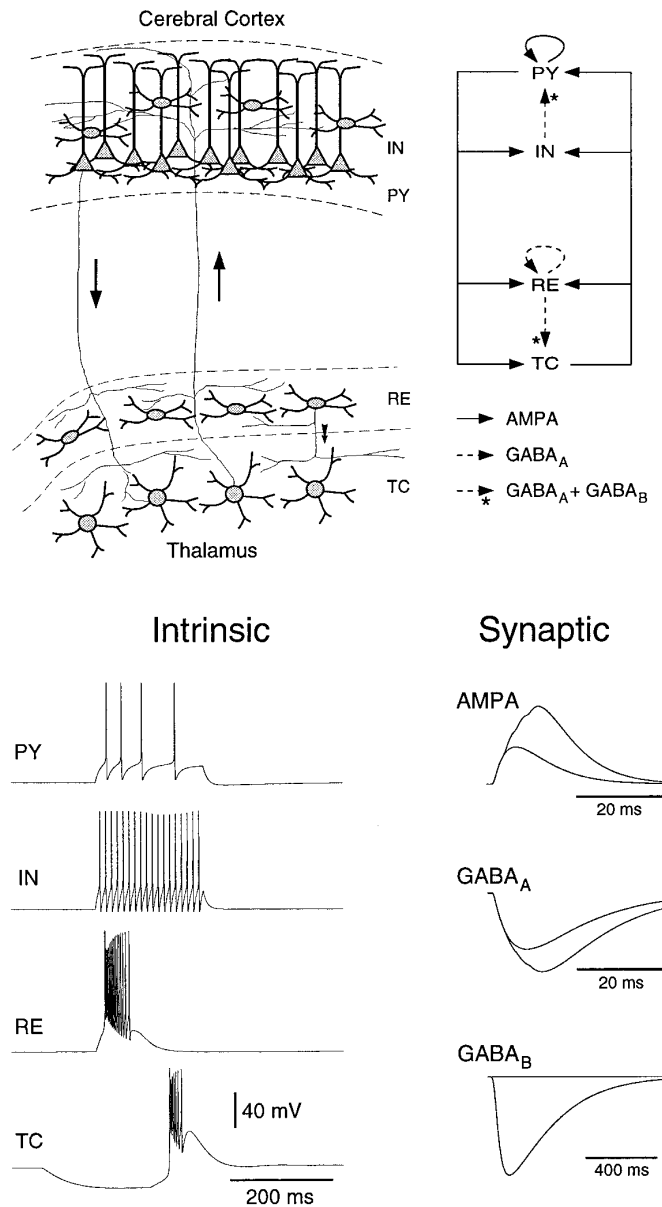

FIG. 1. Connectivity, intrinsic properties and synaptic potentials used in the thalamocortical network model. Four cell types and their connectivity (*top*): thalamocortical (TC) cells, thalamic reticular (RE) neuron, cortical pyramidal cells (PY), and interneurons (IN). *Top right*: connectivity and receptor types used in the model. *Bottom left*: intrinsic firing patterns of 4 cell types: regular-spiking PY cell (depolarizing pulse of 0.75 nA during 200 ms; −70 mV rest), fast spiking IN (same pulse), RE cell burst (pulse of 0.3 nA during 10 ms), and rebound burst in a TC cell (pulse of −0.1 nA during 200 ms). *Bottom right*: time course of postsynaptic potentials for 3 receptor types used. Response after a single presynaptic spike is superimposed to summation of a burst of presynaptic spikes at high frequency (300–400 Hz; 4 spikes for α-amino-3-hydroxy-5-methyl-4-isoxazolepropionic acid (AMPA) and γ-aminobutyric acid-A (GABA$_A$), 10 spikes for GABA$_B$).

Our observations are compatible with previous intracellular recordings in vivo. First, the dominance of inhibition has been previously observed in various thalamic relay neurons after stimulation of related cortical area (Ahlsen et al. 1982; Burke and Sefton 1966; Contreras and Steriade 1996; Deschênes and Hu 1990; Lindström 1982; Roy et al. 1984; Steriade et al. 1972; Widen and Ajmone Marsan 1960).
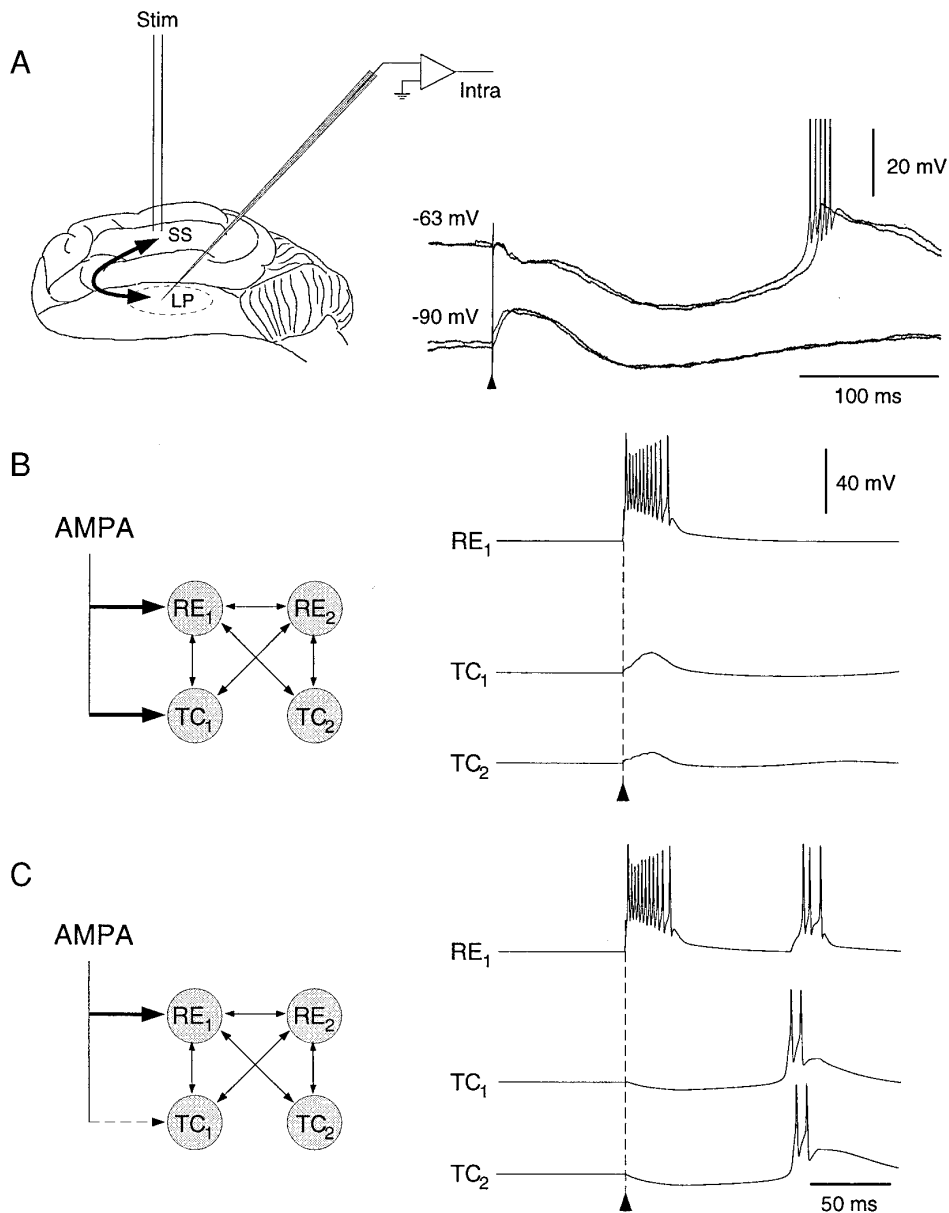
FIG. 2. Cortical stimulation affects thalamic relay cells predominantly through inhibition. *A*: intracellular recording of a TC cell in lateral posterior thalamic nucleus while stimulating anatomically the related part of suprasylvian cortex in cats during barbiturate anesthesia. Cortical stimulation (▲) evoked a small excitatory postsynaptic potential (EPSP) followed by a powerful biphasic inhibatory postsynaptic potential (IPSP). IPSP gave rise to rebound burst in that TC cell. This case was representative of the majority of recorded TC cells. *B*: simulation of cortical EPSPs (AMPA-mediated) in a circuit of 4 interconnected thalamic cells. Cortical EPSPs were stimulated by delivering a presynaptic burst of 4 spikes at 200 Hz to AMPA receptors. Maximal conductance was similar in TC and RE cells (100 nS in this case) and no rebound occurred after stimulation (▲). *C*: same simulation with dominant IPSP in TC cell. In this case, the AMPA conductance of stimulated EPSPs in TC cell was dropped down to 5 nS. Stimulation of AMPA receptors evoked a small EPSP followed by strong IPSP, then by a rebound burst in TC cells, as observed experimentally.

Second, this EPSP-IPSP sequence is transformed into a more powerful EPSP after lesioning the RE nucleus (Deschênes and Hu 1990; Steriade and Deschênes 1988). Third, spindle oscillations can be robustly evoked by stimulating the cortex (even contralaterally to avoid backfiring of TC axons and collateral activation of RE cells, see Contreras and Steriade 1996; Roy et al. 1984; Steriade et al. 1972). Fourth, during spontaneous oscillations, TC cells are entrained into the oscillation by an initial IPSP but rarely by initial EPSPs (Steriade and Deschênes 1984). Fifth, dominant IPSPs were also observed with other anesthetics, such as ketamine-xylazine (Timofeev et al. 1996).

IPSP dominance is optimal to trigger thalamic oscillations

Consistent with the above observations, 9–11 Hz spindle oscillations could be initiated in the model from either intrinsic mechanisms (Fig. 3, *A–B*), or from electrical stimulation of cortical pyramidal cells (Fig. 3, *C–D*). In the first case,

a spontaneous oscillation started from intrinsic oscillatory properties of one of the two TC cells (TC$_1$ in Fig. 3, *A–B*). In the second case, electrical stimulation of a PY cell could evoke spindle oscillations with all TC cells entrained into the oscillation by an initial IPSP (Fig. 3, *C–D*). As described for the thalamic circuit (Fig. 2, *B–C*), cortically evoked rebound burst in TC cells could be observed only if cortical feedback operated on TC cells through dominant inhibition. In the circuit, this property implements the possibility of cortical discharges to evoke oscillations.

The strength of cortical EPSPs on TC cells had an important effect on the network activity. For weak EPSPs, TC cells were dominated by IPSPs from RE cells and cortical discharges efficiently recruited spindle oscillations in the thalamus. When EPSPs and IPSPs were of comparable strength (as in Fig. 2*B*), no oscillation could be evoked from the cortex, because of shunt effect of mixed EPSPs and IPSPs. With further increase in EPSP strength, cortical discharges could evoke spikes in TC cells directly. In this
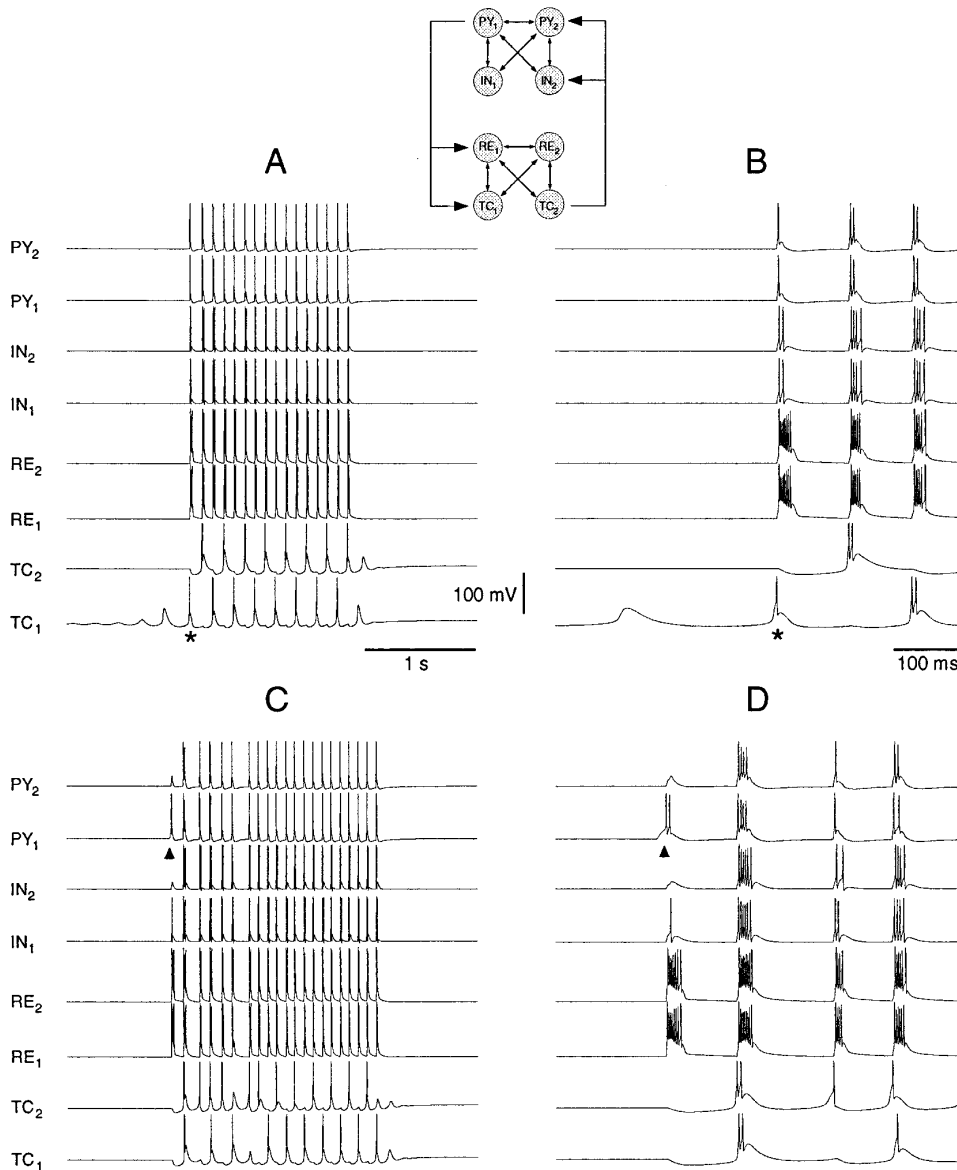
FIG. 3. Simplified thalamocortical circuit for spindle oscillations. Two cells of each type were connected according to diagram (*inset*). Small arrows: bidirectional coupling with receptor types shown in Fig. 1. Large arrows: thalamocortical connectivity, with each PY cell connecting all thalamic cells and each TC cell connecting all cortical cells. *A*: spontaneous spindle oscillation in the circuit. Oscillation began in one TC cell (TC₁, *) and subsequently recruited rest of circuit. Oscillations stopped because of upregulation of I_h in TC cells. *B*: detail at about 10 times higher temporal resolution. *C*: oscillations evoked by electrical stimulation of one PY cell (PY₁—▲). *D*: detail at about 10 times higher temporal resolution. In all cases, spindle oscillations could occur in the circuit only if reticular IPSPs dominated cortical feedback EPSPs in TC cells.

case, sustained spiking of all cell types occurred in the network.

If oscillations were spontaneous or evoked by an initial cortical discharge, the network displayed spindles with similar characteristics: *1*) the frequency range was of 9–11 Hz; *2*) within one cycle, all cell types discharged in phase, as observed experimentally for anatomically related cortical and thalamic territories (Contreras and Steriade 1996); in this case, the rebound burst of TC cells started these in-phase discharges; *3*) because of the moderate rate of discharges of the cells, all IPSPs were dominated by GABA_A whereas GABA_B-mediated currents were minimal; and *4*) the bursting pattern of thalamic cells was similar as in model thalamic circuits without cortical cells, with TC cells bursting once every two cycles (Destexhe et al. 1996a).

The domain of spindle oscillations in conductance parameter space is given in Table 2 (last column). The model was extremely robust to changes in conductance parameters within the range indicated. The condition was that the model generated spindle oscillations that could be initiated by two mechanisms: intrinsic oscillatory behavior in TC cells and cortical stimulation. To fulfill this condition, one critical element was that corticothalamic feedback had to be strong on RE cells but weak on TC cells, in agreement with Fig. 2*C*. The same parameter domain was also valid for larger networks with some restriction (see below; see also details in METHODS).

In larger networks with 100 cells of each type (Fig. 4*A*), the intrinsic connectivity in the thalamus and the cortex was made by using axonal projections over 11 cells, similarly to our previous study of thalamic networks (Destexhe et al. 1996a). Projections between thalamus and cortex were more divergent, consistent with anatomic studies (Jones 1985). I_h conductance values were randomly distributed among TC cells across the network such that several TC cells were spontaneous oscillators (Destexhe et al. 1996a) and served as initiation sites from where the oscillation spread to the whole network. In these conditions, and for a large range of
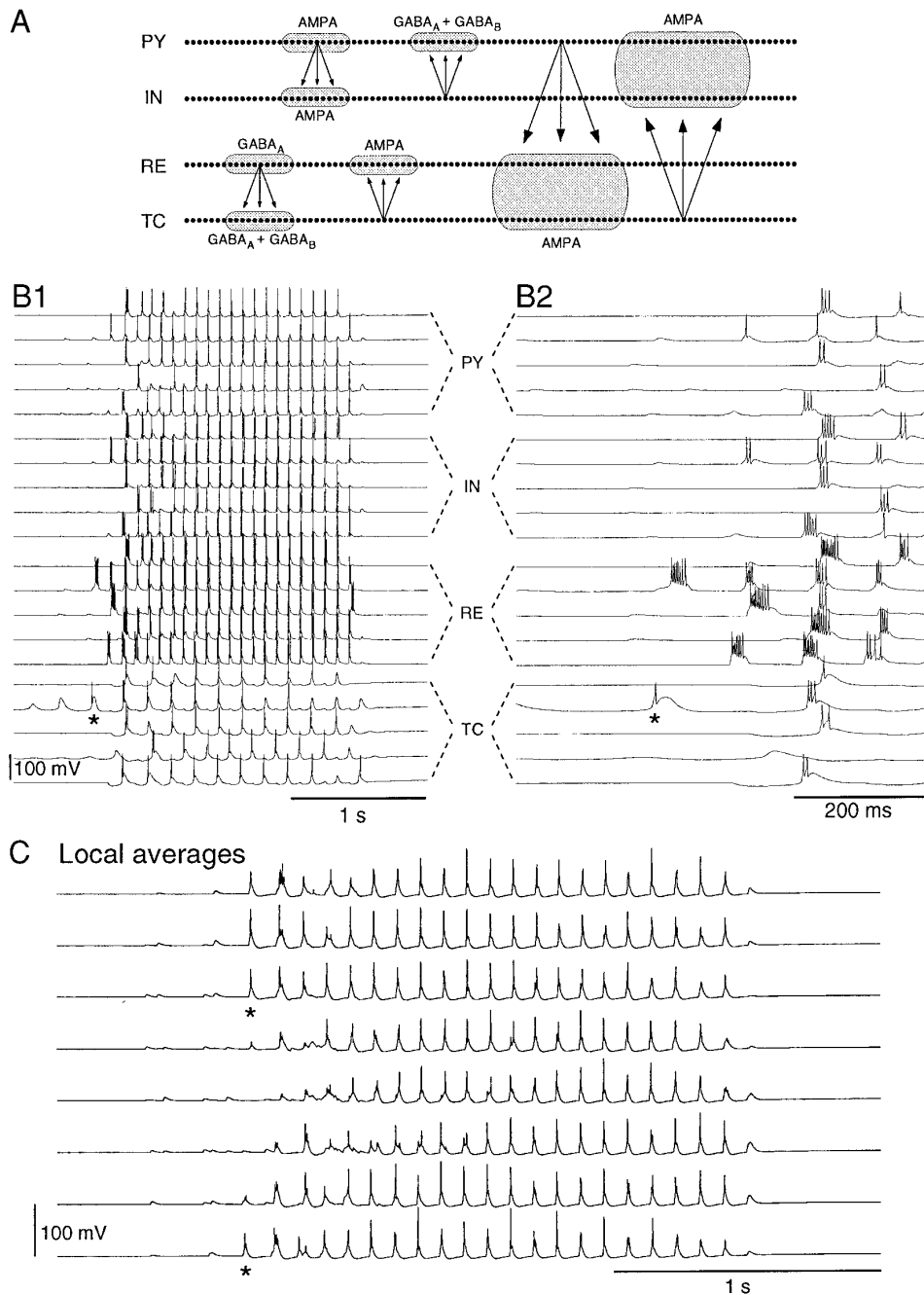
FIG. 4. Spontaneous spindle oscillations in a model thalamocortical network of 400 cells. *A*: scheme of connectivity. The network had 4 layers of PY, IN, RE, and TC cells. Each cell is represented by a dot and the area to which it projects is shown as a shaded area for an example of each type of connection. Intrathalamic and intracortical connections were local using a divergence of 11 cells, whereas thalamocortical and corticothalamic projections were more extended, spanning over 21 cells. *B1*: spontaneous spindle oscillation. Five cells of each type, equally spaced in network, are shown (0.5-ms time resolution). *, an initiator TC cell. *B2*: detail of initiation of spindle. *C*: local average potentials. Twenty-one adjacent PY cells, taken at 8 equally spaced sites on network, were used to calculate each average. *, 2 nearly simultaneous initiation sites.

parameter values, the network generated spindle oscillations with similar cellular discharge patterns as in the simple circuit (Fig. 4*B*).

It must be noted that this oscillation was nearly simultaneous in the sense that the network oscillated in unison during most of the spindle sequence. However, close scrutiny to single-cell behavior (Fig. 4*B*, *1* and *2*) reveals propagating patterns of discharges for cells at neighboring sites, separated by about 100 ms in some cases, similar to observations in multielectrode studies of the cortex and thalamus in vivo (Verzeano and Negishi 1960; Verzeano et al. 1965). However, there was no systematic propagation (as defined in the INTRODUCTION), as these propagating patterns were local in both time and space. Besides these local patterns of propagation, a prominent feature of these oscillations is that the

network came quickly (<500 ms) to a state where the entire system oscillated in unison.

Local average membrane potentials were constructed to compare the network activity with multisite field potentials recordings. In the model, each average trace represents the average over 21 adjacent PY cells. Different averages were taken at eight equally spaced cortical sites on the network. Local averaged potentials showed that the spindle oscillation began approximately simultaneously in several sites (Fig. 4*C*, *). The oscillations then propagated to the entire network and, after one or two cycles, merged into a unique synchronized oscillation. This scheme is similar to the "collision" of spindle waves described in vitro (Kim et al. 1995). However, the mechanisms present here are different from thalamic slices. The main difference is that the synchro-

nization of different foci of oscillations occurs here through corticothalamic interactions, which bypass the prived intrathalamic synchronizing mechanism and set the network in a state of full synchrony within a few cycles.

In average membrane potentials (Fig. 4C), the initiation of the oscillation occurred in different sites within time windows of ~0.2 s, similar to the patterns seen in field potential recordings during barbiturate anesthesia (compare Fig. 4C with Fig. 2 in Contreras et al. 1996a). Also similar to barbiturate anesthesia, successive spindle sequences showed a considerable variability in their initiation pattern, with occurrences of 1–3 near-simultaneous initiation sites. Possible mechanisms for initiation sites to occur nearly simultaneously are described in more detail in the next section.

IPSP dominance determines thalamic coherence

To investigate how cortical feedback can organize the coherence of oscillations in the thalamus, as found experimentally (Contreras et al. 1996a), we investigated the behavior of model thalamic networks. The most striking feature was that individual thalamic cells as well as local average potentials were considerably more simultaneous in the presence of cortical feedback (Fig. 5). The *left panel* shows several spindle sequences using the same parameters as in Fig. 4. The *right panel* shows the same simulation with cortical cells removed. Without cortical feedback, different initiation sites for spindles were not coordinated. Some of them remained local, some others gave rise to systematic propagation of oscillations from side to side of the network (Fig. 5, *bottom right*). Here again, the randomly distributed I_h conductance among TC cells was responsible for this diversity of behavior, because several TC cells were spontaneous oscillators and served as initiation sites.

In this case again, cortical feedback had to recruit TC cells through inhibition to produce this effect. The presumed mechanism is a ''reset'' of the modulation mechanisms of I_h giving rise to the waxing and waning patterns. The IPSP-dominated synaptic feedback is an ideal mechanism to recruit I_h in TC cells. During spindle oscillations starting with such synchronized cortical feedback, the individual upregulation mechanisms of I_h in TC cells tend to synchronize such that several TC cells restart oscillating at roughly the same time, leading to several near-simultaneous initiation sites for spindles.

We tested this idea by performing simulations with variable refractoriness in TC cells. For this purpose, all TC cells had identical I_h and were all initiators (see METHODS). Only the decay rate of I_h modulation was randomized, such that initiator TC cells had silent periods distributed between 4 and 20 s. In such conditions, the thalamocortical network still displayed the typical waxing and waning oscillations, but the pattern was more irregular, with increased occurrence of local oscillations and initiation at multiple sites only occurred exceptionally (not shown). This indicates that the waxing and waning structure of spindles does not depend on a perfect uniformity of refractoriness properties in TC cells, but that uniformity is optimal for different sites to restart oscillating at roughly the same time. Unlike conductance values, which may vary from cell to cell because they depend on the density of channels in the membrane, the length of the silent period is not expected to undergo cell-to-
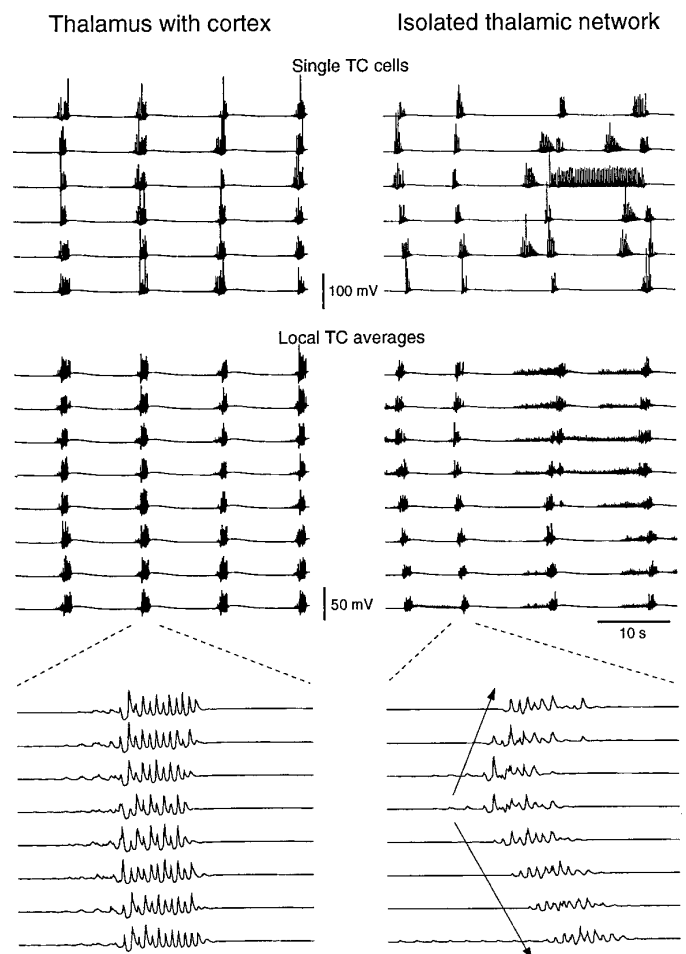

FIG. 5. Simultaneity of spindle oscillations in model thalamic networks is critically dependent on corticothalamic feedback. Spontaneous spindles are shown in the presence of cortex (*left*) and in an isolated thalamic network (*right*) taken in the same conditions (same parameters as in Fig. 4). Single TC cells and local TC averages are shown for each case. Twenty-one adjacent TC cells, taken at 8 equally spaced sites on network, were used to calculate each average. *Bottom*: averages of a representative spindle at 10 times higher temporal resolution. Near simultaneity of oscillations in the presence of cortex is contrasting with patterns of systematic propagation in the isolated thalamic network (arrows).

cell variations because they depend on kinetic rate constants, which are likely to be identical in all cells possessing the same biochemical mechanism. It seems therefore plausible that different TC cells have similar silent periods.

A series of additional properties are consistent with experimental data. First, dual intracellular recordings showed that although there is diminished spatiotemporal coherence in decorticated animals, local synchrony is still present in TC cells located within less than ~1–2 mm (Contreras et al. 1996a; Timofeev and Steriade 1996). The same phenomenon was indeed observed in the model as neighboring TC cells had more synchrony than distant ones (not shown). In models (Destexhe et al. 1996b; Golomb et al. 1996), this effect was the result of the divergence of intrathalamic reciprocal connections between TC and RE cells (Jones 1985).

Second, the spatiotemporal patterns of activity in the model were very similar to experimental data. Spatiotemporal maps of activity from the model (Fig. 6) show that oscillations initiated at different sites for each spindle se-

quence. In the presence of the cortex (Fig. 6, *top left*), initiation occurred in a relatively narrow time window, with sometimes two initiation sites starting at roughly the same time. Without cortex (Fig. 6, *top right*), initiation sites led to local patterns of propagation and colliding waves. In some instances, in the isolated thalamic network, when only a single site of initiation started oscillating, the model produced systematic propagation of spindle waves (last spindle sequence in Fig. 6). These properties of systematic propagation and colliding waves were similar to that found experimentally in thalamic slices (Kim et al. 1995).

Differences in spatiotemporal coherence were also apparent from the presence of horizontal yellow stripes in maps from the thalamic network with cortex, which were not present in maps of the isolated thalamic network (compare color panels in Fig. 6). Power spectrum analyses (not shown) showed that the 7–15 Hz power increases concomitantly in distant sites in the presence of the cortex but not in decorticate animals (similar to Fig 2 in Contreras et al. 1996a). The difference in spatiotemporal coherence was also apparent from spatial correlations. Similar to experiments, spatial correlations from thalamic cells showed a more pronounced decay with distance when cortical feedback was removed compared to the intact thalamocortical network (Fig. 6, *bottom*).

Refractoriness restrains the timing of corticothalamic feedback

A critical property to determine the spatiotemporal properties of thalamic oscillations is the refractoriness of the network. In thalamic slices, spindle oscillations are followed by a period of several seconds during which the thalamic network is refractory to further oscillations (Kim et al. 1995). This property was modeled here as a Ca^{2+}-dependent modulation of I_h (see METHODS). As the decay rate of this upregulation of I_h is very slow, spindle oscillations are followed by a refractory period of several seconds. If the same mechanism is present in the thalamocortical network, it would predict that the cortex can trigger thalamic oscillations only after some period of silence.

This property is indeed observable in thalamocortical networks. In the range of stimulation amplitudes that elicited spindle waves, repetitive cortical shocks showed clear evidence for refractoriness (Fig. 7A). This corroborates our previous observation that cortical stimulation not always produced spindle waves (Contreras et al. 1997a). Indeed, oscillations could be evoked by cortical stimulation only if a period of silence preceded the stimulation by ~2–8 s, depending on stimulation intensity. In Fig. 7A, stimuli delivered at moderate intensity at a period of 4 s entrained the whole network once every two stimuli. This indicates that, for that stimulus intensity, the refractory period is >8 s but <12 s. Similar values were measured in ferret thalamic slices (Kim et al. 1995).

In the model, refractoriness was also observable through cortical stimulation (Fig. 7B). The refractory period was of ~10 s, similar to experiments (Fig. 7A). In this model, refractoriness was the result of Ca^{2+}-dependent upregulation of I_h in TC cells, similarly to a previous model of thalamic slices (Destexhe et al. 1996a). The model therefore shows that refractoriness confines the cortical triggering action to a short time window at the end of the interspindle lull.

Refractoriness determines propagating properties

Spontaneous spindle waves show patterns of systematic propagation in ferret thalamic slices (Kim et al. 1995). Their properties could be explained by upregulation of I_h and the topographical structure of reciprocal connections between TC and RE cells (Destexhe et al. 1996a). Systematic propagation of spontaneous oscillations are, however, not observed in vivo, as oscillations show variable initiation patterns with no systematic delay (Andersen and Andersson 1968). However, spindles evoked by low-intensity cortical stimulation in vivo can show patterns of systematic propagation with an apparent higher velocity (Fig. 10 in Contreras et al. 1997a).

In the model, systematic propagation of spindle waves could be evoked by delivering depolarizing current pulses of random amplitude simultaneously to a localized population of PY cells (10 adjacent cells—Fig. 8, Local). The initial discharge in a localized population of cortical cells recruited a local population of thalamic cells through excitation of the RE nucleus (same mechanism as in Fig. 3D). TC cells then produced rebound bursts that reexcited a larger population of cortical cells and the same cycle restarted, leading to the progressive invasion of the network. Similar systematic propagation patterns could be evoked by stimulation of either TC, RE, or PY cells (not shown).

The model accounts for two additional features of cortically evoked oscillations. First, oscillations evoked by high intensity do not show patterns of systematic propagation but are nearly simultaneous (Contreras et al. 1997a). In the model, the spatial extent of the stimulation was increased by stimulating cells distributed through the network (1 of 10 cells). In this case, although the same number of cells were stimulated, the stimulus gave nearly simultaneous spindle oscillation in the entire system (Fig. 8, Extended), suggesting that high-intensity cortical stimulation discharges a more extended population of cortical cells. Second, systematic propagation patterns resist transection of horizontal intracortical connections (Contreras et al. 1997a). The characteristics of evoked oscillations in the model also resisted interruption of corticocortical connections (Fig. 8, Localcut), identically to experiments (compare with Fig. 11 in Contreras et al. 1997a).

From Fig. 8A, the propagation velocity was of about 600 ms for a spatial scale of 100 cells in the network. A simulation performed with a network of a twice larger number of cells (200 neurons of each type), with axonal projections extending to twice the size described in METHODS, gave rise to systematic propagation with a velocity of ~600 ms for 200 cells. In this case, the twice wider axonal projections gave a twice larger absolute velocity, but the velocity was the same if expressed in % of the size of the network. This simulation shows that the propagation velocity and therefore the velocity of generalization of the oscillation, does not depend on the absolute number of cells in the network but rather on the relative size of axonal projections compared to the total size of the network.

In conclusion, the model suggests the following scenario depending on the presence of thalamic refractoriness. First, patterns of systematic propagation can be generated at the end of the refractory period by exciting a localized area of the thalamus. This localized excitation is reproduced by

localized low-intensity cortical stimulation. Second, the synchronization after high-intensity cortical stimulation is due to the activation of a more extended population of cortical cells at once. Third, the systematic propagation of evoked spindles in the cortex is due to the reciprocal corticothalamic connectivity and not to horizontal intracortical connections.

Spontaneous cortical discharges control spatiotemporal properties

The refractory period of spindle waves in vivo has approximately the same duration as the period of oscillations occurring spontaneously (4–10 s). In contrast, in thalamic slices, the refractory period (5–10 s) is shorter than the period of spontaneous oscillations (10–20 s; Kim et al. 1995). In a model of thalamic slices (Destexhe et al. 1996b), the refractory period was also shorter than spontaneous oscillation period. This effect was due to the fact that, after recovery from refractoriness, the network ''waited'' for a spontaneous event to occur to trigger the next spindle wave.

We hypothesize that, because of the higher level of spontaneous activity in vivo, spindle sequences are initiated as soon as the network has recovered from refractoriness. Again, the initiation of thalamic oscillations by the cortex plays an essential role here. This effect could be simulated with the model if cortical PY cells were subject to random synaptic bombardment such that they fire occasionally (Fig. 9). In this case, successive oscillatory sequences occurred from the occasional discharge of cortical PY cells (Fig. 9A, ∗) through a mechanism of recruitment involving the cortical feedback onto the thalamus, similar to Fig. 3D.

Several properties of these spontaneous spindles were strikingly similar to in vivo recordings: 1) the period was in the range of 4–10 s; 2) there was a great variability in the period; 3) local spindles occurred occasionally. Local spindles were triggered when spontaneous cortical discharges occurred before complete recovery from refractoriness, which corroborates the shorter silent period that precedes local spindles in vivo (D. Contreras, A. Destexhe, and M. Steriade, unpublished observations).

DISCUSSION

In this paper, we have provided a hypothetical mechanism to explain the spatiotemporal properties and distribution of spindle oscillations in the thalamocortical system. We discuss here the plausibility of this mechanism, how it accounts for both in vivo and in vitro data on these oscillations, and what predictions are generated to test its validity.

Corticothalamic feedback on RE cells

The main prediction of the model is that the synchronizing influence of the corticothalamic feedback is due to IPSP dominance in TC cells. We have provided experimental evidence for dominant IPSPs in lateral posterior TC cells after cortical stimulation during barbiturate anesthesia (Fig 2A). This feature is consistent with previous in vivo observations, which consistently reported that cortical stimulation evokes responses in TC cells dominated by inhibition (Ahlsen et al. 1982; Burke and Sefton 1966; Contreras and Steriade 1996; Contreras et al. 1996b; Deschênes and Hu 1990; Lindström 1982; Roy et al. 1984; Steriade et al. 1972; Widen and

Ajmone Marsan 1960). Stimulation of the internal capsule in thalamic slices (Thomson and West 1991) or cortical stimulation in thalamocortical slices (Kao and Coulter 1997) also reported EPSP-IPSP sequences dominated by inhibition in a significant proportion of the recorded TC cells. It could be argued, however, that we overestimated the dominance of IPSPs over EPSPs because of the effect of barbiturate anesthetics. This is unlikely since barbiturates do not influence neither the peak nor the rise time of GABAergic currents but they only prolong their decay (Thompson 1994), which should not mask an early EPSP.
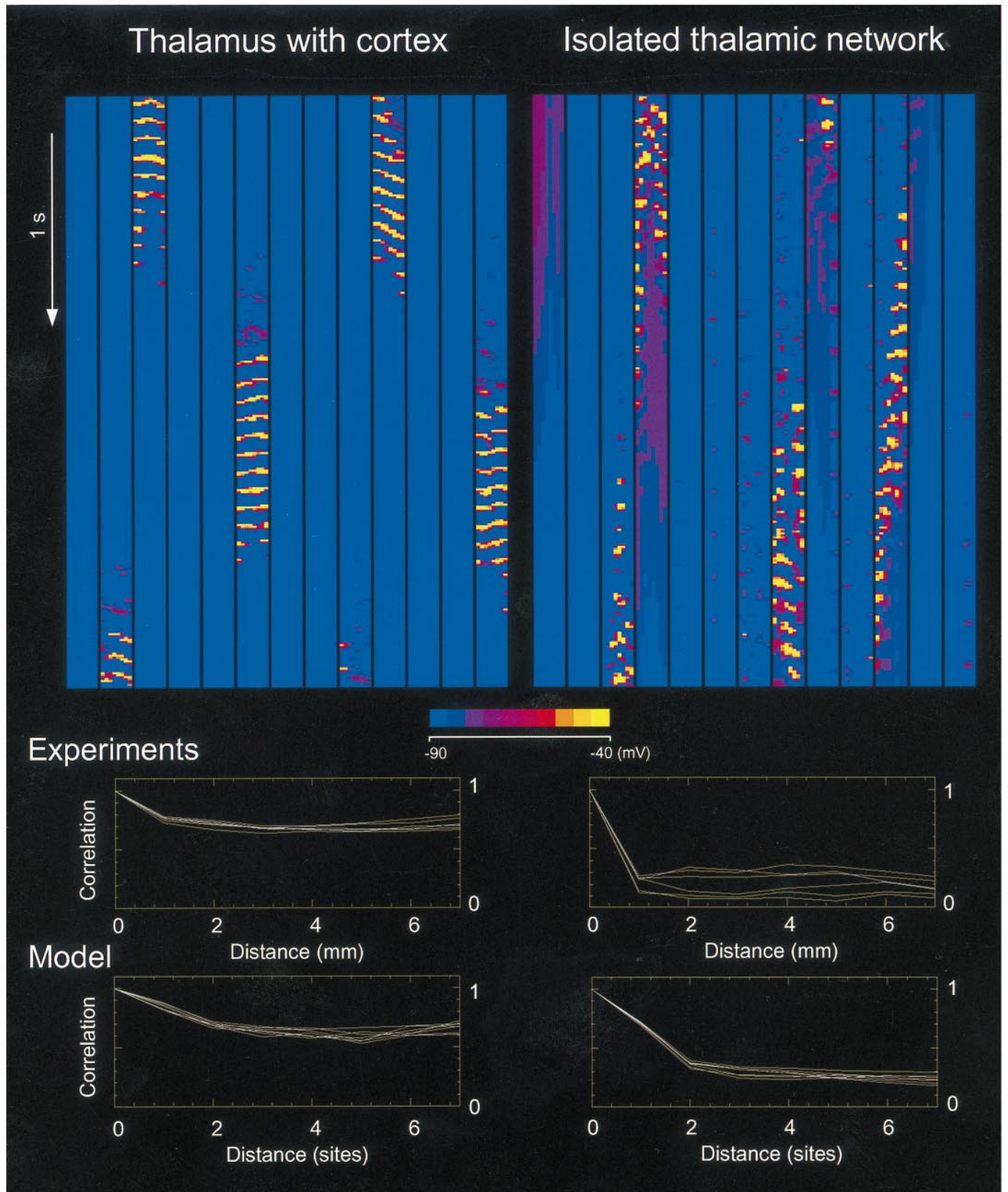
Several additional features are consistent with IPSP dominance in TC cells. First, cortical synapses on TC cells end on the most distal part of the dendritic tree, whereas inhibitory synapses from the RE nucleus are more proximal (Erisir et al. 1997a; Liu et al. 1995). Consequently, cortical EPSPs are likely to be shunt by reticular IPSPs, leading to dominant IPSP in the soma. Second, a large part of synaptic terminals in the thalamus (lateral geniculate) arise from brainstem structures, which leaves much fewer cortical synapses on TC cells than previously thought (Erisir et al. 1997b). Third, TC cells are usually entrained into oscillations through an initial IPSP (Steriade and Deschênes 1984). Fourth, during cortical seizure activity, a significant proportion (60%) of TC cells are hyperpolarized, while cortical cells produce paroxysmal discharges leading to strong excitation of RE cells (Steriade and Contreras 1995). Finally, the fact that RE cells may have a powerful dendritic T-current (Destexhe et al. 1996b) would make their dendrites very sensitive to cortical EPSPs. Consistent with this, IPSPs are seen in TC cells even with low-intensity cortical stimuli (D. Contreras and M. Steriade, unpublished observations). It may be that implementing such a sensitivity of RE cells to cortical EPSPs is one of the reason explaining the presence of T-current in their dendrites.

The model also shows that no thalamic oscillations can be evoked if cortical EPSPs on TC cells are too strong (Fig. 2B). This suggests that the most optimal way of recruiting thalamic circuits into oscillations is by exciting RE cells. Experiments are consistent with this condition, as cortical stimulation is a very effective way of evoking low-frequency thalamic oscillations (Contreras and Steriade 1996; Roy et al. 1984; Steriade et al. 1972).

A cellular mechanism for large-scale synchrony in cortex

As spindle oscillations are generated in the thalamus, it was initially suggested that synchrony in the thalamocortical system depends exclusively on intrathalamic mechanisms (Andersen and Andersson 1968). However, the powerful role of the cortex in triggering spindling must be taken into account (Morison and Dempsey 1943; Steriade et al. 1972). Recent experiments (Contreras et al. 1996a, 1997a) established that the large-scale synchrony of oscillations in the thalamocortical system does not depend on intrathalamic mechanisms, but required the presence of the cortex. In the present paper, we have presented a cellular mechanism to account for the large-scale synchrony of oscillations on the basis of interactions between thalamus and cortex. The model proposes answers to several questions about different experimental aspects of these oscillations.

Why do spontaneous spindle waves appear in different sites at approximately the same time in vivo (Contreras et al.

A

Experiments

B

Model

FIG. 7. Refractoriness of thalamic circuits is observable through cortical stimulation. *A*: refractoriness of spindle oscillations evoked by cortical stimulation during barbiturate anesthesia. *Top*: electrode setup for multisite field potential recordings in cat suprasylvian cortex (SS, suprasylvian gyrus; ES, ectosylvian gyrus; M, marginal gyrus; PC, postcruciate gyrus). *Bottom*: field potential recordings in cortex during repetitive cortical stimulation. Stimuli were repeated every 4 s through a stimulating electrode located adjacent to electrode 8. *B*: refractoriness of spindle oscillations in the model. *Top*: illustration of the 8 equidistant sites chosen to calculate local average membrane potentials of PY cells. *Bottom*: local average potentials during cortical stimulation of PY cells repeated every 4 s. Pyramidal cells (1 out of 5) were stimulated by injecting current pulses with random amplitude (0–1 nA) and random duration (0–100 ms). (– – –), stimulus onset.
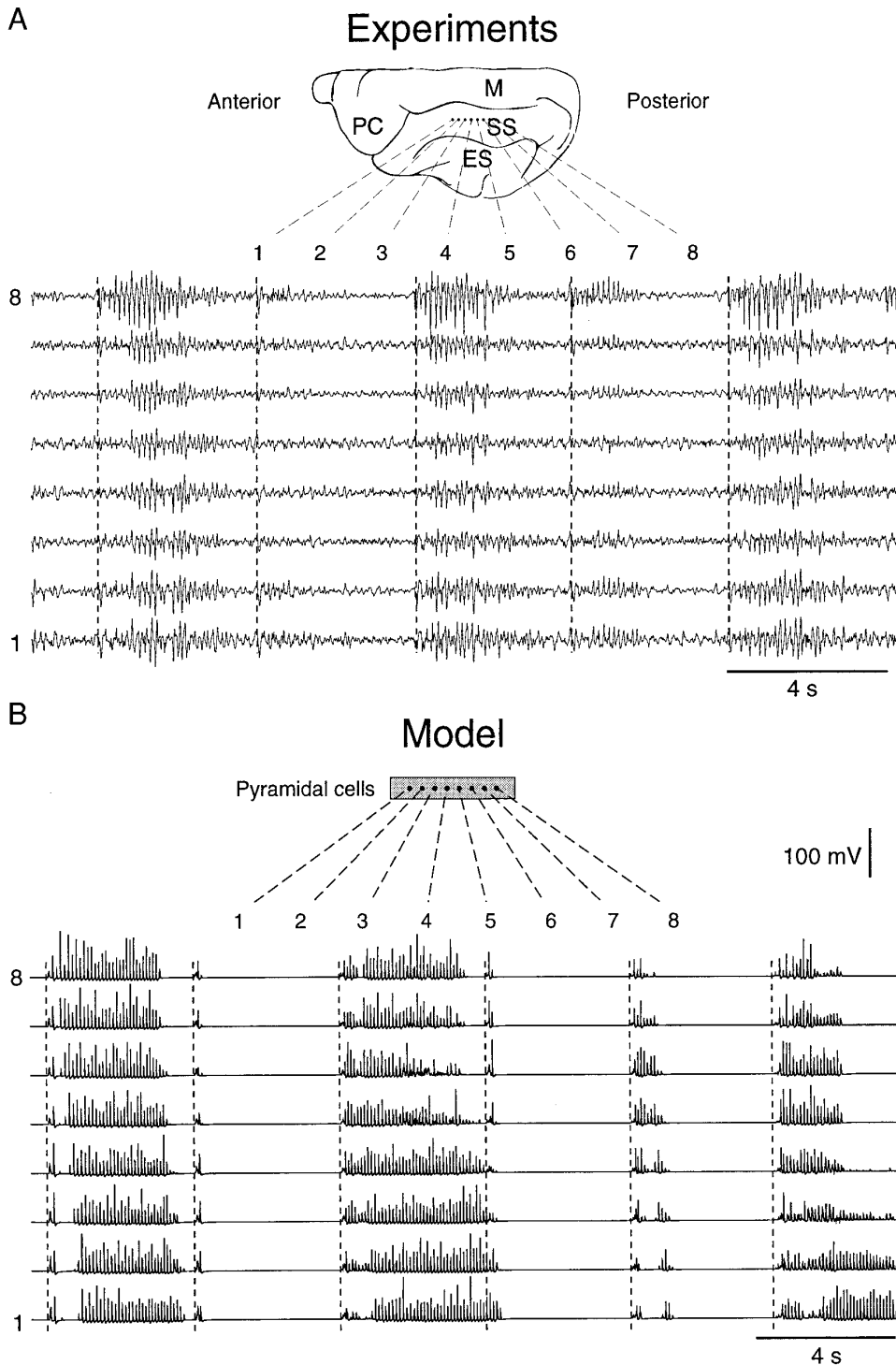
FIG. 6. Presence of cortical feedback determines spatiotemporal coherence of oscillations in model thalamic networks. *Top*: spatiotemporal maps were constructed from local TC averages of spontaneous spindles in presence of cortex (*left*) and in an isolated thalamic network with same parameters (*right*). Each frame consisted of a horizontal stripe of 8 color spots representing membrane potential of TC averages shown in Fig. 5. Frames were arranged from top to bottom in 13 columns (a total of 40 s of activity is shown). Colors ranged in 10 steps from −90 or below (blue) to −40 mV or above (yellow; see color scale). Same simulations and average procedures as in Fig. 5. *Bottom*: decay of correlation with distance. Crosscorrelations were computed for all possible pairs of sites and value at time zero from each correlation was represented as a function of intersite distance. Experiments: decay of correlations of thalamic local field potentials in intact (*left*) and decorticate (*right*) cats under barbiturate anesthesia (modified from Contreras et al., 1996b). Model: decay of correlation calculated for local averaged potentials in presence of cortex (*left*) and in isolated thalamic network (*right*).

Local   Extended   Local - cut
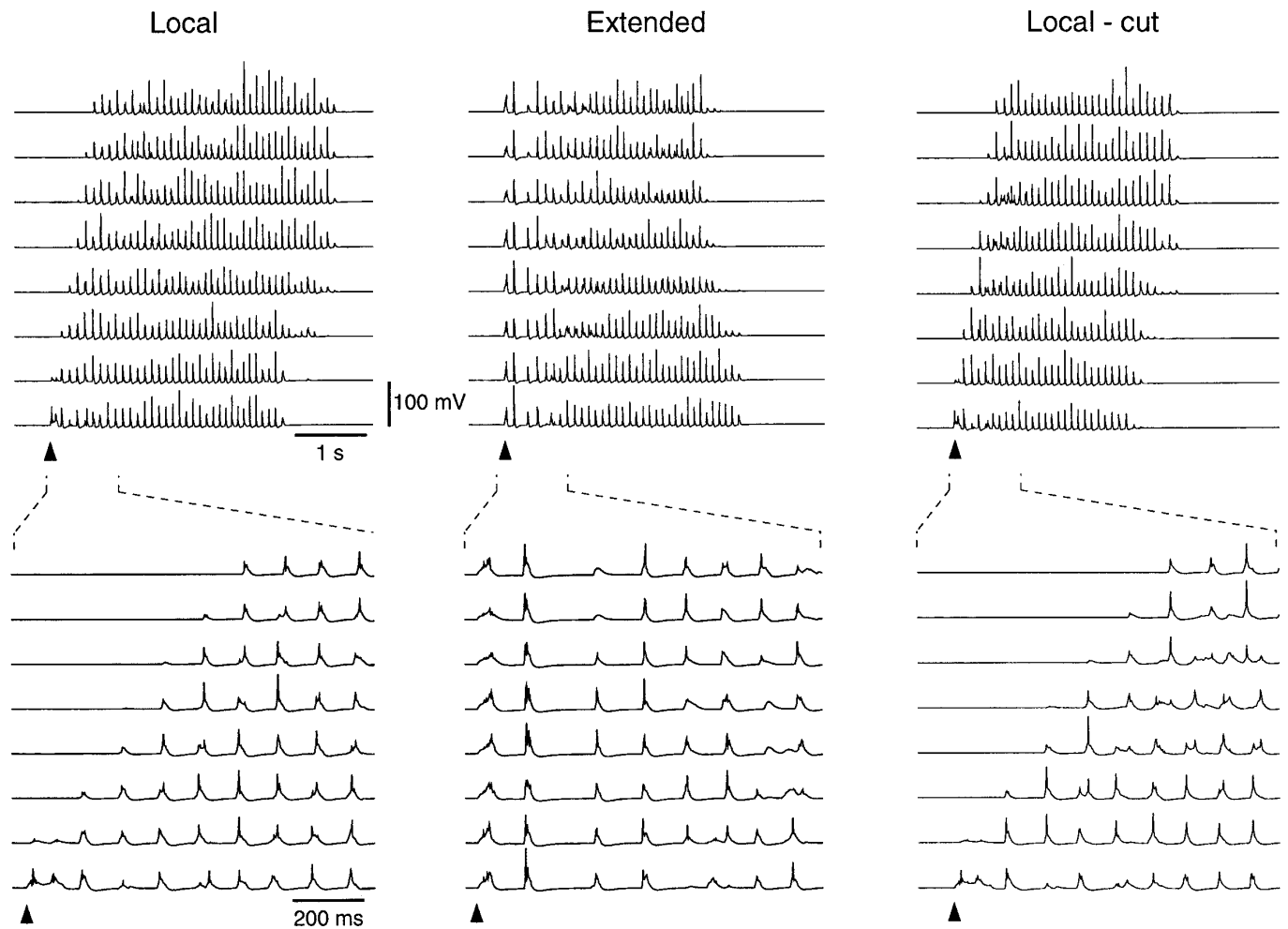

FIG. 8.   Patterns of systematic propagation and nearly simultaneous spindle oscillations can be evoked by stimulating cortical cells in the model. *Top*: local average potentials of PY cells (same procedures and parameters as in Fig. 4). *Bottom*: a detail of beginning of oscillatory sequence (5-times higher temporal resolution). Local: stimulation of 10 adjacent pyramidal cells evoked a spindle oscillation that propagated away from the stimulus site. Extended: stimulation of 1 out of 5 pyramidal cells evoked a nearly simultaneous oscillation. Local-cut: local stimulation with cortical cut produced patterns of systematic propagation similar to local stimulation in the intact network. The cut consisted in a suppression of all connections crossing a virtual line at half of the network. Stimuli were injected current pulses with random amplitude (0–1 nA) and random duration (0–100 ms). ▲, stimulus onset.

1997a), whereas they typically show patterns of systematic propagation in thalamic slices (Kim et al. 1995)? The present model suggests that these differences are primarily due to synchronization mechanisms that involve corticothalamic loops rather than intrathalamic loops (Fig. 10), but they need to act through the RE nucleus (thalamocorticoreticular loops). These loops are very efficient to synchronize large areas because the divergence of different axonal projection systems must be added (cortex-to-RE, RE-to-TC, TC-to-cortex). In addition, the presence of refractory period in TC cells leads to the possibility that spindles that may initiate during the same time period at multiple sites. Several initiation sites then lead to oscillations that generalize over the entire network within a few cycles. Thalamic slices are deprived from this powerful synchronizing system and show systematic propagation through the topographic structure of intrathalamic connections (Fig. 10A; see Destexhe et al. 1996a).

What mechanisms underlly multiple initiation sites? Under the hypothesis that refractoriness is due to a modulation of

I_h by calcium (Destexhe et al. 1996a), the length of the refractory period depends on biochemical rate constants that are likely to be similar in all TC cells that possess this mechanism. Therefore, the refractory period is likely to be the same on average throughout the thalamocortical system, such that initiator TC cells will tend to restart oscillating at roughly the same time. The result is that several nearly simultaneous initiation sites are likely to occur in large thalamic networks, which should lead to increased simultaneity of oscillations. Therefore, the presence of similar refractory periods throughout the thalamocortical system is a very efficient mechanism to promote large-scale synchrony.

Why low-intensity cortical stimulation can nevertheless evoke systematic propagation of oscillations in vivo (Contreras et al. 1997a)? We interpret the contrasting occurrence of systematic propagation after low-intensity cortical stimuli by a "bypass" of these nearly simultaneous initiation sites. A localized cortical area is stimulated before the thalamus had restarted to oscillate, "forcing" a propagating oscillation through the topographic structure of the network. Simi-
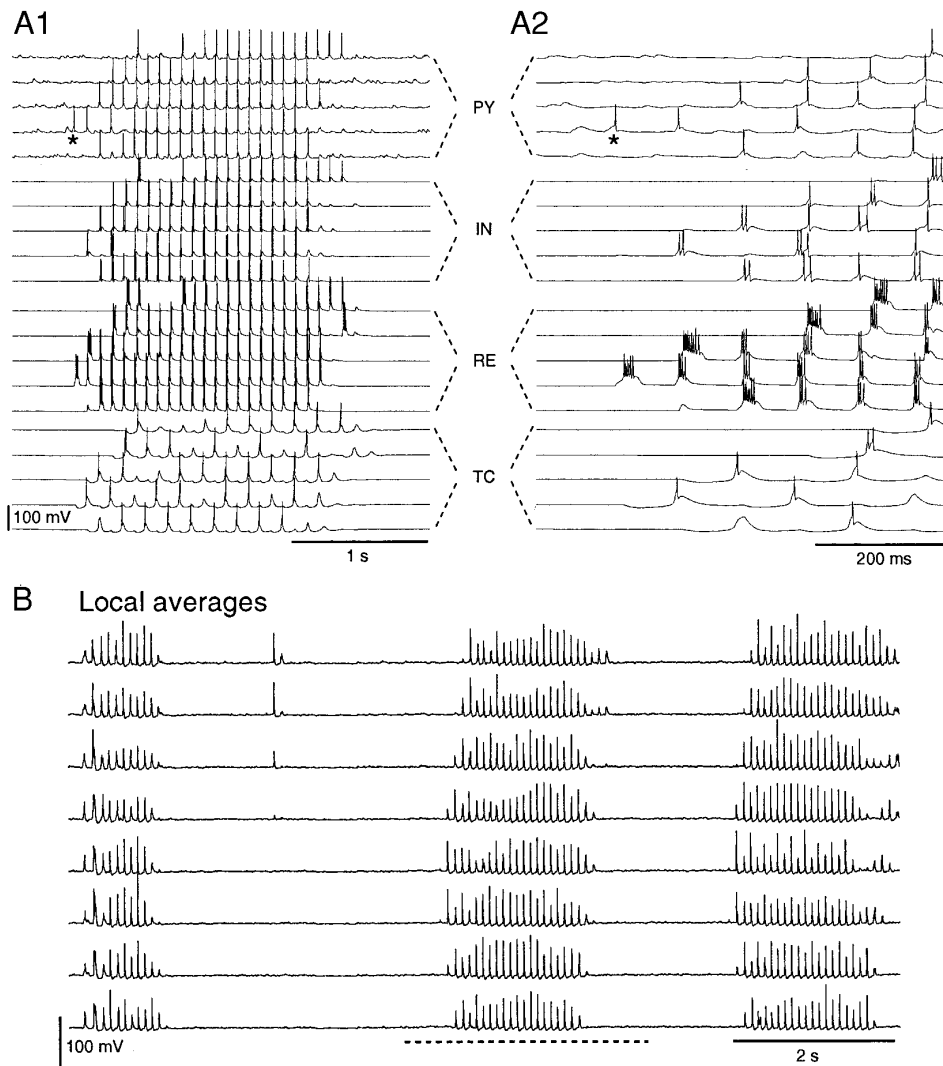
A1

A2

PY

IN

RE

TC

100 mV

1 s

200 ms

FIG. 9. Random discharges of cortical pyramidal cells leads to more noisy patterns of spontaneous spindle oscillations. Same parameters and description as Fig. 4, except that every PY cell had 40 extra synapses (20 AMPA and 20 GABA$_A$), which received random presynaptic action potentials (details in METHODS). *A1*: spontaneous spindle oscillation in single cells. Five cells of each type equally spaced in network are shown (same description as in Fig. 4*B*). Spindle oscillation started by the spontaneous discharge of a PY cell (∗). *A2*: detail of initiation of spindle wave. *B*: local average membrane potentials of PY cells. Spontaneous spindle oscillations were highly variable with periods in the range of 4–10 s.

B   Local averages

100 mV

2 s

larly, cortical stimulation could reveal the refractoriness of the network by ''bypassing'' intrinsic initiations of oscillations (Fig. 7).

What underlies the high variability patterns of spindles in vivo (Andersen and Andersson 1968; Andersen et al. 1967)? One of the prominent features of spindle oscillations is that they are efficiently triggered by cortical stimulation (Contreras and Steriade 1996; Roy et al. 1984; Steriade et al. 1972). This feature was present in the model and oscillations were not necessarily initiated in the thalamus, but could start from one or several cortical sites. In some cases, a cortical discharge occurred when the network had not totally recovered from refractoriness and local oscillations appeared. Cortical discharges may occur as soon as the network recovered from refractoriness, again bypassing intrinsic initiation mechanisms of the thalamus. The result is that such an active network will display more complex patterns of spindles, with interspindle periods of the same order of magnitude as the refractory period, as we observed here.

What mechanisms underlie the large-scale synchrony over distant cortical areas? The present mechanism is compatible with the measurement of large-scale synchrony made in area 5–7 of cat cerebral cortex during barbiturate anesthesia (Andersen and Andersson 1968; Contreras et al. 1997a). How-

ever, spindles occurring during natural sleep seem to have a higher degree of coherence (Contreras et al. 1997a,b). To account for synchrony over distant cortical areas, interareal connections must be taken into account, such as for example corticothalamic axons that project to several thalamic nuclei (Bourassa and Deschênes 1995). Another possibility is the more diffuse connectivity of the rostral pole of the RE nucleus (Steriade et al., 1984), which may account for the occasional occurrence of nearly simultaneous oscillations in the decorticated thalamus (see Fig. 8, panel 2 in Contreras et al. 1997b). More detailed characterization and further modeling studies would be needed to address this point.

In conclusion, the model emphasizes the important role of refractoriness of thalamic circuits, as evidenced in thalamic slices (Bal and McCormick 1996; Kim et al. 1995). The model suggests a mechanism in which thalamocortical loops interact with these refractoriness properties to produce spatiotemporal patterns of spindle oscillations, such as their waxing-waning structure, their variability and their large-scale synchrony across the thalamocortical system.

Predictions

First, relating the extent of axonal projections to the propagation velocity provides a prediction about their size. In

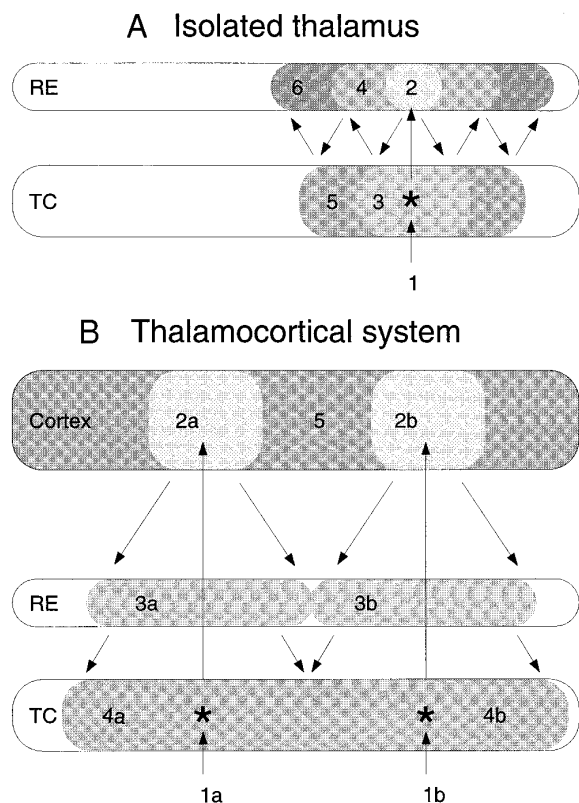## A   Isolated thalamus

B   Thalamocortical system

FIG. 10. Mechanisms of large-scale synchrony in thalamocortical systems. *A*: synchronization mechanisms in isolated thalamus following a mutual recruitment of thalamocortical (TC) relay cells and thalamic reticular (RE) cells. From an initial discharge of a TC cell (1; *), a localized area of RE cells is recruited (2), which in turn recruit a larger area of TC cells (3), etc. Progressively larger areas of thalamus are recruited at each successive cycles (4, 5, 6, . . .) through topographic structure of connectivity. An array or electrodes would record a ''systematic propagation'' of oscillation, such as found in thalamic slices (Kim et al., 1995). *B*: postulated recruitment mechanism in presence of cortex. Two approximately simultaneous initiation sites in thalamus (1a, 1b) recruit localized cortical areas (2b, 2c), which in turn recruit connected areas of RE nucleus (3a, 3b), which in turn recruit larger areas in TC cells (4a, 4b), etc. At the next cycle, the entire cortical area is recruited (5). In this case, corticothalamic connections supersede ''prived'' thalamic recruitment mechanisms shown in *A* and oscillations attain a state of large-scale synchrony within few cycles, consistent with in vivo data (Contreras et al. 1996a).

the model, the propagation velocity was proportional to the addition of TC-to-cortex, cortex-to-RE, RE-to-TC axonal projections. As the propagation velocity is similar between the model and experiments (compare Fig. 8 with Fig 10 in Contreras et al. 1997a), the intersite distance of 11 cells, used to calculate the averages in Fig. 8, roughly corresponds to the interelectrode distance of 1 mm in the experiments. Assuming that similarity, the size of the thalamocortical projections in the cortical network (21 cells in Fig. 4*A*) would correspond to a predicted size of 1.9 mm in the cortex. Although this predicted size for thalamocortical arborizations in cortical area 5–7 is fairly large, it is consistent with the current estimates in somatosensory cortex, reporting that ascending TC axons extend to ~600 μm, with neighboring TC cells projecting up to 1500 μm (Landry and Deschênes 1981; Rausell and Jones 1995).

To scale the model up to real networks, one cell would correspond to a population extending on ~90 μm diam in cortex (1 mm/11), or about 315 cortical neurons (assuming

a density of 100,000 neurons per mm^3). In the thalamus, it was estimated before that 11 neurons is roughly equivalent to 200 μm in the slice (Destexhe et al. 1996a). Therefore, a thalamic cell in the model represents a volume of about 20 μm diam in the thalamus. The ensemble of axons from TC cells in this volume project to the cortex, contacting neurons within an area of a diameter of about 1900 μm (90 × 21). Similarly, a group of cells within 90 μm diam in cortex send their axons that ramify within a diameter of ~380 μm in the thalamus. These size of projections are within the range of experimental measurements (Bourassa and Deschênes 1995; Freund et al. 1989; Landry and Deschênes 1981; Rausell and Jones 1995).

Second, the important role for IPSP dominance given in this study also leads to several predictions. If IPSP dominance determines spatiotemporal coherence, then local injections of GABA$_A$ blockers in thalamic relay nuclei should lead to dramatic changes in the large-scale coherence of oscillations. A similar effect would be obtained by preventing RE cells to fire bursts. This mechanism could be also tested by local application of synaptic channel antagonists in slices: the ability of corticothalamic axons to evoke thalamic oscillations should be unchanged by blocking excitatory synapses on TC cells; on the other hand, it should be profoundly altered by blocking GABA$_A$-mediated inhibition in TC cells.

Third, the present model leads to a general prediction about corticothalamic interactions. It provides evidence that the recruitment of the thalamic circuitry through the RE nucleus is a plausible mechanism to evoke and maintain oscillations with long-range synchrony in the whole thalamocortical system. This mechanism is consistent with the long-range synchrony observed in the cortex for slow oscillations during deep sleep but contrasts with the local synchrony of fast oscillations (20–60 Hz) observed during activated periods (Steriade and Amzica 1996; Steriade et al. 1996). To allow local synchrony, the present model indicates that the corticothalamic feedback must act in an opposite way, by recruiting TC cells with dominant EPSPs and weak IPSPs (not shown). It may be that the dual cholinergic effect on thalamic cells (depolarization of TC cells but hyperpolarization of RE cells; see McCormick 1992) implements a switch between two different types of thalamic responsiveness. In the bursting mode, the corticothalamic feedback would recruit bursts in RE cells, therefore dominant IPSPs in TC cells, leading to long-range synchrony. In activated states, cholinergic modulation would setup a different mode, preventing bursts in RE cells (Hu et al. 1989), therefore favoring EPSPs on TC cells, compatible with local synchrony and relay of information to the cerebral cortex.

REFERENCES

AHLSEN, G., GRANT, K., AND LINDSTRÖM, S. Monosynaptic excitation of principal cells in the lateral geniculate nucleus by corticofugal fibers. *Brain Res.* 234: 454–458, 1982.

ANDERSEN, P. AND ANDERSSON, S. A. *Physiological Basis of the Alpha Rhythm.* New York: Appelton Century Crofts, 1968.

ANDERSEN, P. AND SEARS, T. A. The role of inhibition in phasing of spontaneous thalamo-cortical discharge. *J. Physiol. (Lond.)* 173: 459–480, 1964.

ANDERSEN, P., ANDERSSON, S. A., AND LOMO, T. Nature of thalamocortical relations during spontaneous barbiturate spindle activity. *J. Physiol. (Lond.)* 192: 283–307, 1967.

AVENDAÑO, C., RAUSELL, E., PEREZ-AGUILAR, D., AND ISORNA, S. Organization of the association cortical afferent connections of area 5: a retrograde tracer study in the cat. *J. Comp. Neurol.* 278: 1–33, 1988.

AVENDAÑO, C., RAUSELL, E., AND REINOSO-SUAREZ, F. Thalamic projections to areas 5a and 5b of the parietal cortex in the cat: a retrograde horseradish peroxidase study. *J. Neurosci.* 5: 1446–1470, 1985.

BAL, T. AND MCCORMICK, D. A. What stops synchronized thalamocortical oscillations? *Neuron* 17: 297–308, 1996.

BAL, T., VON KROSIGK, M., AND MCCORMICK, D. A. Synaptic and membrane mechanisms underlying synchronized oscillations in the ferret LGNd in vitro. *J. Physiol. (Lond.)* 483: 641–663, 1995a.

BAL, T., VON KROSIGK, M., AND MCCORMICK, D. A. Role of the ferret perigeniculate nucleus in the generation of synchronized oscillations in vitro. *J. Physiol. (Lond.)* 483: 665–685, 1995b.

BOURASSA, J. AND DESCHÊNES, M. Corticothalamic projections from the primary visual cortex in rats: a single fiber study using biocytin as an anterograde tracer. *Neuroscience* 66: 253–263, 1995.

BREMER, F. Cerebral and cerebellar potentials. *Physiol. Rev.* 38: 357–388, 1958.

BUDDE, T., BIELLA, G., MUNSCH, T., AND PAPE, H. C. Lack of regulation by intracellular Ca^{2+} of the hyperpolarization-activated cation current in rat thalamic neurones. *J. Physiol. (Lond.)* 503: 79–85, 1997.

BURKE, W. AND SEFTON, A. J. Inhibitory mechanisms in lateral geniculate nucleus of rat. *J. Physiol. (Lond.)* 187: 231–246, 1966.

CONNORS, B. W. AND GUTNICK, M. J. Intrinsic firing patterns of diverse neocortical neurons. *Trends Neurosci.* 13: 99–104, 1990.

CONTRERAS, D., CURRÓ DOSSI, R., AND STERIADE, M. Electrophysiological properties of cat reticular thalamic neurones in vivo. *J. Physiol. (Lond.)* 470: 273–294, 1993.

CONTRERAS, D., DESTEXHE, A., SEJNOWSKI, T. J., AND STERIADE, M. Control of spatiotemporal coherence of a thalamic oscillation by corticothalamic feedback. *Science* 274: 771–774, 1996a.

CONTRERAS, D., DESTEXHE, A., SEJNOWSKI, T. J., AND STERIADE, M. Spatiotemporal patterns of spindle oscillations in cortex and thalamus. *J. Neurosci.* 17: 1179–1196, 1997a.

CONTRERAS, D., DESTEXHE, A., AND STERIADE, M. Spindle oscillations during cortical spreading depression in naturally sleeping cats. *Neuroscience* 77: 933–936, 1997b.

CONTRERAS, D. AND STERIADE, M. Cellular bases of EEG slow rhythms: a study of dynamic corticothalamic relationships. *J. Neurosci.* 15: 604–622, 1995.

CONTRERAS, D. AND STERIADE, M. Spindle oscillation in cats: the role of corticothalamic feedback in a thalamically-generated rhythm. *J. Physiol. (Lond.)* 490: 159–179, 1996.

CONTRERAS, D., TIMOFEEV, I., AND STERIADE, M. Mechanisms of longlasting hyperpolarizations underlying slow sleep oscillations in cat corticothalamic networks. *J. Physiol. (Lond.)* 494: 251–264, 1996b.

CURRÓ DOSSI, R., NUNEZ, A., AND STERIADE, M. Electrophysiology of a slow (0.5–4 Hz) intrinsic oscillation of cat thalamocortical neurones in vivo. *J. Physiol. (Lond.)* 447: 215–234, 1992.

DESCHÊNES, M. AND HU, B. Electrophysiology and pharmacology of the corticothalamic input to lateral thalamic nuclei: an intracellular study in the cat. *Eur. J. Neurosci.* 2: 140–152, 1990.

DESTEXHE, A., BABLOYANTZ, A., AND SEJNOWSKI, T. J. Ionic mechanisms for intrinsic slow oscillations in thalamic relay neurons. *Biophys. J.* 65: 1538–1552, 1993a.

DESTEXHE, A., BAL, T., MCCORMICK, D. A., AND SEJNOWSKI, T. J. Ionic mechanisms underlying synchronized oscillations and propagating waves in a model of ferret thalamic slices. *J. Neurophysiol.* 76: 2049–2070, 1996a.

DESTEXHE, A., CONTRERAS, D., SEJNOWSKI, T. J., AND STERIADE, M. A model of spindle rhythmicity in the isolated thalamic reticular nucleus. *J. Neurophysiol.* 72: 803–818, 1994a.

DESTEXHE, A., CONTRERAS, D., SEJNOWSKI, T. J., AND STERIADE, M. Modeling the control of reticular thalamic oscillations by neuromodulators. *NeuroReport* 5: 2217–2220, 1994b.

DESTEXHE, A., CONTRERAS, D., STERIADE, M., SEJNOWSKI, T. J., AND HUGUENARD, J. R. In vivo, in vitro and computational analysis of dendritic calcium currents in thalamic reticular neurons. *J. Neurosci.* 16: 169–185, 1996b.

DESTEXHE, A., MAINEN, Z. F., AND SEJNOWSKI, T. J. An efficient method for computing synaptic conductances based on a kinetic model of receptor binding. *Neural Comput.* 6: 14–18, 1994c.

DESTEXHE, A., MAINEN, Z. F., AND SEJNOWSKI, T. J. Kinetic models of synaptic transmission. In: *Methods in Neuronal Modeling (2nd ed.)*, edited by C. Koch and I. Segev. Cambridge, MA: MIT Press, 1998, p. 1–26.

DESTEXHE, A., MCCORMICK, D. A., AND SEJNOWSKI, T. J. A model for 8–10 Hz spindling in interconnected thalamic relay and reticularis neurons. *Biophys. J.* 65: 2474–2478, 1993b.

DESTEXHE, A. AND SEJNOWSKI, T. J. G-protein activation kinetics and spillover of GABA may account for differences between inhibitory responses in the hippocampus and thalamus. *Proc. Natl. Acad. Sci. USA* 92: 9515–9519, 1995.

ERISIR, A., VANHORN, S. C., AND SHERMAN, S. M. Relative numbers of cortical and brainstem inputs to the lateral geniculate nucleus. *Proc. Natl. Acad. Sci. USA* 94: 1517–1520, 1997a.

ERISIR, A., VANHORN, S. C., BICKFORD, M. E., AND SHERMAN, S. M. Immunocytochemistry and distribution of parabrachial terminals in the lateral geniculate nucleus of the cat: a comparison with corticogeniculate terminals. *J. Comp. Neurol.* 377: 535–549, 1997b.

FITZGIBBON, T., TEVAH, L. V., AND JERVIE-SEFTON, A. Connections between the reticular nucleus of the thalamus and pulvinar-lateralis posterior complex: a WGA-HRP study. *J. Comp. Neurol.* 363: 489–504, 1995.

FREUND, T. F., MARTIN, K. A., SOLTESZ, I., SOMOGYI, P., AND WHITTERIDGE, D. Arborisation pattern and postsynaptic targets of physiologically identified thalamocortical afferents in striate cortex of the macaque monkey. *J. Comp. Neurol.* 289: 315–336, 1989.

GOLOMB, D., WANG, X. J., AND RINZEL, J. Synchronization properties of spindle oscillations in a thalamic reticular nucleus model. *J. Neurophysiol.* 72: 1109–1126, 1994.

GOLOMB, D., WANG, X. J., AND RINZEL, J. Propagation of spindle waves in a thalamic slice model. *J. Neurophysiol.* 75: 750–769, 1996.

HAGIWARA, N. AND IRISAWA, H. Modulation by intracellular Ca^{2+} of the hyperpolarization—activated inward current in rabbit single sino-atrial node cells. *J. Physiol. (Lond.)* 409: 121–141, 1989.

HERSCH, S. M. AND WHITE, E. L. Thalamocortical synapses on corticothalamic projections neurons in mouse SmI cortex: electron microscopic demonstration of a monosynaptic feedback loop. *Neurosci. Lett.* 24: 207–210, 1981.

HINES, M. L. AND CARNEVALE, N. T. The NEURON simulation environment. *Neural Computat.* 9: 1179–1209, 1997.

HODGKIN, A. L. AND HUXLEY, A. F. A quantitative description of membrane current and its application to conduction and excitation in nerve. *J. Physiol. (Lond.)* 117: 500–544, 1952.

HU, B., STERIADE, M., AND DESCHÊNES, M. The effects of brainstem peribrachial stimulation on perigeniculate neurons: the blockage of spindle waves. *Neuroscience* 31: 1–12, 1989.

HUGUENARD, J. R. AND MCCORMICK, D. A. Simulation of the currents involved in rhythmic oscillations in thalamic relay neurons. *J. Neurophysiol.* 68: 1373–1383, 1992.

JAHNSEN, H. AND LLINÁS, R.R. Ionic basis for the electroresponsiveness and oscillatory properties of guinea-pig thalamic neurons in vitro. *J. Physiol. (Lond.)* 349: 227–247, 1984.

JONES, E. G. *The Thalamus.* New York: Plenum, 1985.

KAO, C. Q. AND COULTER, D. A. Physiology and pharmacology of corticothalamic stimulation-evoked responses in rat somatosensory thalamic neurons in vitro. *J. Neurophysiol.* 77: 2661–2676, 1997.

KIM, U., BAL, T., AND MCCORMICK, D. A. Spindle waves are propagating synchronized oscillations in the ferret LGNd in vitro. *J. Neurophysiol.* 74: 1301–1323, 1995.

LANDRY, P. AND DESCHÊNES, M. Intracortical arborizations and receptive fields of identified ventrobasal thalamocortical afferents to the primary somatic sensory cortex in the cat. *J. Comp. Neurol.* 199: 345–371, 1981.

LEGENDRE, P., ROSENMUND, C., AND WESTBROOK, G. L. Inactivation of NMDA channels in cultured hippocampal neurons by intracellular calcium. *J. Neurosci.* 13: 674–684, 1993.

LERESCHE, N., LIGHTOWLER, S., SOLTESZ, I., JASSIK-GERSCHENFELD, D., AND CRUNELLI, V. Low frequency oscillatory activities intrinsic to rat and cat thalamocortical cells. *J. Physiol.* 441: 155–174, 1991.

LINDSTRÖM, S. Synaptic organization of inhibitory pathways to principal cells in the lateral geniculate nucleus of the cat. *Brain Res.* 234: 447–453, 1982.

LIU, X. B., HONDA, C. N., AND JONES, E. G. Distribution of four types of synapse on physiologically identified relay neurons in the ventral posterior thalamic nucleus of the cat. *J. Comp. Neurol.* 352: 69–91, 1995.

LUTHI, A. AND MCCORMICK, D. A. Both electrophysiological and biochemical oscillations determine spindle wave rhythmicity. *Soc. Neurosci. Abstr.* 23: 1820, 1997.

MCCORMICK, D. A. Neurotransmitter actions in the thalamus and cerebral cortex and their role in neuromodulation of thalamocortical activity. *Prog. Neurobiol.* 39: 337–388, 1992.

MCCORMICK, D. A. AND HUGUENARD, J. R. A model of the electrophysiological properties of thalamocortical relay neurons. *J. Neurophysiol.* 68: 1384–1400, 1992.

MCCORMICK, D. A. AND PAPE, H. C. Properties of a hyperpolarization-activated cation current and its role in rhythmic oscillations in thalamic relay neurones. *J. Physiol. (Lond.)* 431: 291–318, 1990.

MCCORMICK, D. A., WANG, Z., AND HUGUENARD, J. Neurotransmitter control of neocortical neuronal activity and excitability. *Cereb. Cortex* 3: 387–398, 1993.

MINDERHOUD, J. M. An anatomical study of the efferent connections of the thalamic reticular nucleus. *Exp. Brain Res.* 112: 435–446, 1971.

MORISON, R. S. AND BASSETT, D. L. Electrical activity of the thalamus and basal ganglia in decorticate cats. *J. Neurophysiol.* 8: 309–314, 1945.

MORISON, R. S. AND DEMPSEY, E. W. Mechanisms of thalamocortical augmentation and repetition. *Am. J. Physiol.* 138: 297–308, 1943.

MULLE, C., MADARIAGA, A., AND DESCHÊNES, M. Morphology and electrophysiological properties of reticularis thalami neurons in cat: in vivo study of a thalamic pacemaker. *J. Neurosci.* 6: 2134–2145, 1986.

OTIS, T. S. AND MODY, I. Modulation of decay kinetics and frequency of GABA$_A$ receptor-mediated spontaneous inhibitory postsynaptic currents in hippocampal neurons. *Neuroscience* 49: 13–32, 1992.

OTIS, T. S., DE KONICK, Y., AND MODY, I. Characterization of synaptically elicited GABA$_B$ responses using patch-clamp recordings in rat hippocampal slices. *J. Physiol. (Lond.)* 463: 391–407, 1993.

PARÉ, D., CURRÓ DOSSI, R., AND STERIADE, M. Three types of inhibitory postsynaptic potentials generated by interneurons in the anterior thalamic complex of cat. *J. Neurophysiol.* 66: 1190–1204, 1991.

PRESS, W. H., FLANNERY, B. P., TEUKOLSKY, S. A., AND VETTERLING, W. T. *Numerical Recipes. The Art of Scientific Computing.* Cambridge: Cambridge Univ. Press, 1986.

RAUSELL, E. AND JONES, E. G. Extent of intracortical arborization of thalamocortical axons as a determinant of representational plasticity in monkey somatic sensory cortex. *J. Neurosci.* 15: 4270–4288, 1995.

ROBERTSON, R. T. AND CUNNINGHAM, T. J. Organization of corticothalamic projections from parietal cortex in cat. *J. Comp. Neurol.* 199: 569–585, 1981.

ROY, J. P., CLERCQ, M., STERIADE, M., AND DESCHÊNES, M. Electrophysiology of neurons in lateral thalamic nuclei in cat: mechanisms of long-lasting hyperpolarizations. *J. Neurophysiol.* 51: 1220–1235, 1984.

STERIADE, M. AND AMZICA, F. Intracortical and corticothalamic coherency of fast spontaneous oscillations. *Proc. Natl. Acad. Sci. USA* 93: 2533–2538, 1996.

STERIADE, M. AND CONTRERAS, D. Relations between cortical and thalamic cellular events during transition from sleep patterns to paroxysmal activity. *J. Neurosci.* 15: 623–642, 1995.

STERIADE, M., CONTRERAS, D., AMZICA, F., AND TIMOFEEV, I. Synchronization of fast (30–40 Hz) spontaneous oscillations in intrathalamic and thalamocortical networks. *J. Neurosci.* 16: 2788–2808, 1996.

STERIADE, M. AND DESCHÊNES, M. The thalamus as a neuronal oscillator. *Brain Res. Rev.* 8: 1–63, 1984.

STERIADE, M. AND DESCHÊNES, M. Intrathalamic and brainstem-thalamic networks involved in resting and alert states. In: *Cellular Thalamic Mechanisms,* edited by M. Bentivoglio and R. Spreafico, Amsterdam: Elsevier, 1988, p. 51–76.

STERIADE, M., DESCHÊNES, M., DOMICH, L., AND MULLE, C. Abolition of spindle oscillations in thalamic neurons disconnected from nucleus reticularis thalami. *J. Neurophysiol.* 54: 1473–1497, 1985.

STERIADE, M., DOMICH, L., OAKSON, G., AND DESCHÊNES, M. The deafferented reticular thalamic nucleus generates spindle rhythmicity. *J. Neurophysiol.* 57: 260–273, 1987.

STERIADE, M., MCCORMICK, D. A., AND SEJNOWSKI, T. J. Thalamocortical oscillations in the sleeping and aroused brain. *Science* 262: 679–685, 1993a.

STERIADE, M., NUNEZ, A., AND AMZICA, F. Intracellular analysis of relations between the slow (<1 Hz) neocortical oscillation and other sleep rhythms of the electroencephalogram. *J. Neurosci.* 13: 3266–3283, 1993b.

STERIADE, M., PARENT, A., HADA, J. Thalamic projections of nucleus reticularis thalami of cat: a study using retrograde transport of horseradish peroxidase and double fluorescent tracers. *J. Comp. Neurol.* 229: 531–547, 1984.

STERIADE, M., WYZINSKI, P., AND APOSTOL, V. Corticofugal projections governing rhythmic thalamic activity. In: *Corticothalamic Projections and Sensorimotor Activities,* edited by T. L. Frigyesi, E. Rinvik, M. D. Yahr, New York: Raven Press, p. 221–272, 1972.

THOMPSON, S. M. Modulation of inhibitory synaptic transmission in the hippocampus. *Prog. Neurobiol.* 42: 575–609, 1994.

THOMSON, A. M. AND WEST, DC. Local-circuit excitatory and inhibitory connections in slices of the rat thalamus (Abstract). *J. Physiol. (Lond.)* 438: 113, 1991.

TIMOFEEV, I., CONTRERAS, D., AND STERIADE, M. Synaptic responsiveness of cortical and thalamic neurones during various phases of slow sleep oscillation in cat. *J. Physiol. (Lond.)* 494: 265–278, 1996.

TIMOFEEV, I. AND STERIADE, M. The low-frequency rhythms in the thalamus of intact-cortex and decorticated cats. *J. Neurophysiol.* 76: 4152–4168, 1996.

TOTH, T. AND CRUNELLI, V. Modelling spindle-like oscillations in thalamocortical neurones. *Soc. Neurosci. Abstr.* 18: 1018, 1992.

TRAUB, R. D. AND MILES, R. *Neuronal Networks of the Hippocampus.* Cambridge: Cambridge Univ. Press, 1991.

ULRICH, D. AND HUGUENARD, J. R. GABA$_B$ receptor-mediated responses in GABAergic projection neurones of rat nucleus reticularis thalami in vitro. *J. Physiol. (Lond.)* 493: 845–854, 1996.

UPDYKE, B. V. Projections from visual areas of the middle suprasylvian sulcus onto the lateral posterior complex and adjacent thalamic nuclei in cat. *J. Comp. Neurol.* 201: 477–506, 1981.

VERZEANO, M. AND NEGISHI, K. Neuronal activity in cortical and thalamic networks. A study with multiple microelectrodes. *J. Gen. Physiol.* 43: 177–195, 1960.

VERZEANO, M., LAUFER, M., SPEAR, P., AND MCDONALD, S. L'activité des reśeaux neuroniques dans le thalamus du singe. *Actualiteś Neurophysiologiques* 6: 223–251, 1965.

VON KROSIGK, M., BAL, T., AND MCCORMICK, D. A. Cellular mechanisms of a synchronized oscillation in the thalamus. *Science* 261: 361–364, 1993.

WANG, X. J. AND RINZEL, J. Spindle rhythmicity in the reticularis thalami nucleus—synchronization among inhibitory neurons. *Neuroscience* 53: 899–904, 1993.

WHITE, E. L. Termination of thalamic afferents in the cerebral cortex. In: *Cerebral Cortex*, edited by E. G. Jones and A. Peters. New York: Plenum, 1986, Vol. 5, p. 271–289.

WHITE, E. L. AND HERSCH, S. M. A quantitative study of thalamocortical and other synapses involving the apical dendrites of corticothalamic cells in mouse SmI cortex. *J. Neurocytol.* 11: 137–157, 1982.

WIDEN, K. AND AJMONE MARSAN, C. Effects of corticopetal and corticofugal impulses upon single elements of the dorsolateral geniculate nucleus. *Exp. Neurol.* 2: 468–502, 1960.

XIANG, Z., GREENWOOD, A. C., AND BROWN, T. Measurement and analysis of hippocampal mossyfiber synapses. *Soc. Neurosci. Abstr.* 18: 1350, 1992.